UNIVERSITY OF PARDUBICE

FACULTY OF CHEMICAL TECHNOLOGY

Department of analytical chemistry

Marek Svoboda

Adaptation of conventional and modern non-invasive methods for analysis of photoaged human skin barrier

Theses of the Doctoral Dissertation

Pardubice 2020

Study program: **Analytical chemistry**

Study field: **Analytical chemistry**

Author: **Mgr. Marek Svoboda**

Supervisor: **prof. RNDr. Zuzana Bílková, Ph.D.**

Co-Supervisors: **Mgr. Iva Dolečková, Ph.D.**

Mgr. Tomáš Muthný, Ph.D.

Year of the defense: **2020**

References:

SVOBODA, Marek. *Adaptation of conventional and modern non-invasive methods for analysis of photoaged human skin barrier.* Pardubice, 2020, 121 pages. Doctoral thesis. University of Pardubice, Faculty of Chemical Technology, Department of Analytical Chemistry. Supervisor prof. RNDr. Zuzana Bílková, Ph.D.

Abstract:

This doctoral thesis deals with the phenomenon of unchanged or even decreased trans-epidermal water loss (TEWL) in the aged skin despite a decreased skin barrier lipids content. To address this task, analysis of structural components of the skin barrier was performed along with analysis of the skin barrier properties by using a wide range of methods. Optimal procedures for the skin sampling and subsequent sample handling and analysis were established as the first step. The second step included the analysis of the epidermal tight junction (TJ) proteins expression, lipid content and the skin barrier properties in the skin affected by ageing to select a potential target responsible for this phenomenon. The last part of this thesis challenged the target molecule occludin with regard to TEWL in the skin with diminished lipid barrier by using an ex vivo porcine skin model.

Keywords: confocal microscopy, immunochemistry, lipids, PCR, skin barrier, thin-layer chromatography, TEWL, tight junctions

Abstrakt:

Tato dizertační práce se zabývá fenoménem stabilní nebo dokonce snížené transepidermální ztráty vody (TEWL) ve stárnoucí kůži navzdory nižšímu obsahu bariérových lipidů. K řešení této problematiky bylo nutné analyzovat strukturální komponenty kožní bariéry a biofyzikální parametry kůže, k čemuž byla použitá celá řada analytických metod. Jako první krok byla provedena optimalizace postupu pro odběr vzorku a jeho následného zpracování a analýzy. Další krok zahrnoval analýzu exprese proteinů epidermálních těsných spojů, analýzu obsahu lipidů a analýzu bariérových vlastností v kůži ovlivněné stárnutím, což bylo použito k následné selekci možných cílových molekul zodpovědných za výše uvedený fenomén. Poslední část této práce zkoumá potenciální molekulu okludin ve vztahu k TEWL v kůži se sníženým obsahem lipidů za použití ex vivo modelu prasečí kůže.

Klíčová slova: imunochemie, konfokální mikroskopie, kožní bariéra, lipidy, PCR, tenko-vrstevná chromatografie, TEWL, těsné spoje

Table of Contents

1 Introduction

The skin as an external organ creates a crucial barrier in the human body. The barrier function of the skin is fulfilled by its outermost skin layer, the epidermis, where the stratum corneum (SC) plays a key role (Elias 2005; Pouillot et al. 2008; Proksch et al. 2008). The skin as the barrier protects the organism from biological and chemical threats, regulates the passage of molecules and protects against physical insults such as UV-light. However, these external factors damage the skin triggering respective cellular responses which over time cause the skin aging. Up to 90% of the skin aging features may be attributed to the photoaging and its most significant factor, the UV irradiation (Gilchrest 2013; Kohl et al. 2011; Shah and Rawal Mahajan 2013).

The aged skin has a deteriorated barrier function with an altered permeability to various substances (Farage et al. 2008; Hung et al. 2012; Vinson and Anamandla 2006), which is thought to be caused by a decreased lipid content in the SC. More specifically, a generally accepted idea is that the aged skin losses approximately 30% of ceramides (Coderch et al. 2003). Paradoxically, the water barrier does not show any signs of deterioration associated with aging as trans-epidermal water loss (TEWL) remains constant or even decreases with age (Kottner et al. 2013b; Luebberding et al. 2013a; Luebberding et al. 2013b). Although several hypotheses have been introduced, this phenomenon has not been elucidated yet. After an acute damage to the skin barrier either by tape-stripping (TS), organic solvents or by UV-light, TEWL significantly increases in the damaged area and returns to normal after 10 days, even though the SC is not fully recovered suggesting some sort of compensatory mechanism (Jiang et al. 2007; Kottner et al. 2013b; Malminen et al. 2003; Yuki et al. 2011).

The debate puts forward a role of tight junctions (TJs). TJs were shown to be an important contributor to the barrier function of the skin (Kirschner et al. 2013; Yuki et al. 2007). A knockdown or downregulation of most TJ proteins is associated with the barrier dysfunction, as reviewed in (Svoboda et al. 2016). In this regard, TJs have shown the ability to compensate for damaged or even completely missing SC. During this process, some of the TJ proteins such as zonulin (ZO)-1 or occludin exert an increased expression resulting in a blockage of the passage of various molecules at TJ positive sites (Celli et al. 2012; Malminen et al. 2003). We aimed to investigate whether the same mechanism works also in the photoaged skin affected by years of the chronic UV exposure or in the intrinsically aged skin, and whether TJs can regulate TEWL of the photoaged skin or intrinsically aged skin in such manner. We analyzed TEWL, lipid composition and organization, and expression of claudin-1, occludin and ZO-2 in the young and aged, both sun-protected (volar) and sun-exposed (dorsal) forearm skin.

Such an approach requires a sampling from various skin regions. Due to regional epidermal differences, the sampling techniques must be flexible and performable almost anywhere on the skin area (Sandby-Møller et al. 2003; Tagami 2008). A few techniques, invasive and non-invasive, are used for the skin sampling, where punch biopsy dominates as a quick and reliable technique providing a substantial amount of a full-thickness skin sample. However, punch biopsy represents a painful intervention into the body causing a permanent skin damage and brings along the potential health risks such as infection, nerve damage or allergy to anesthetics, which should not be neglected

(Nischal et al. 2008; Zuber 2002). Moreover, punch biopsy must be performed by an acknowledged physician. Altogether, punch biopsy is highly demanding on research laboratories to meet the ethics committee requirements, and thus research laboratories might find it rather difficult to acquire a biopsy of intended both quality and quantity. Therefore, techniques with minimalized invasiveness such as suction blistering (SB) and TS, which are less painful and leave no permanent damage (Serup et al. 2006), are more suitable for common research laboratories. Generally, SB and TS techniques do not provide full-thickness skin samples, which is not imperative for the epidermal analysis. However, it is a question what the possibilities and limits of these techniques for the analysis of the epidermis are. To ensure reliable analysis of epidermal lipids and TJ proteins, reproducible sampling process and detection methods must be established and optimized.

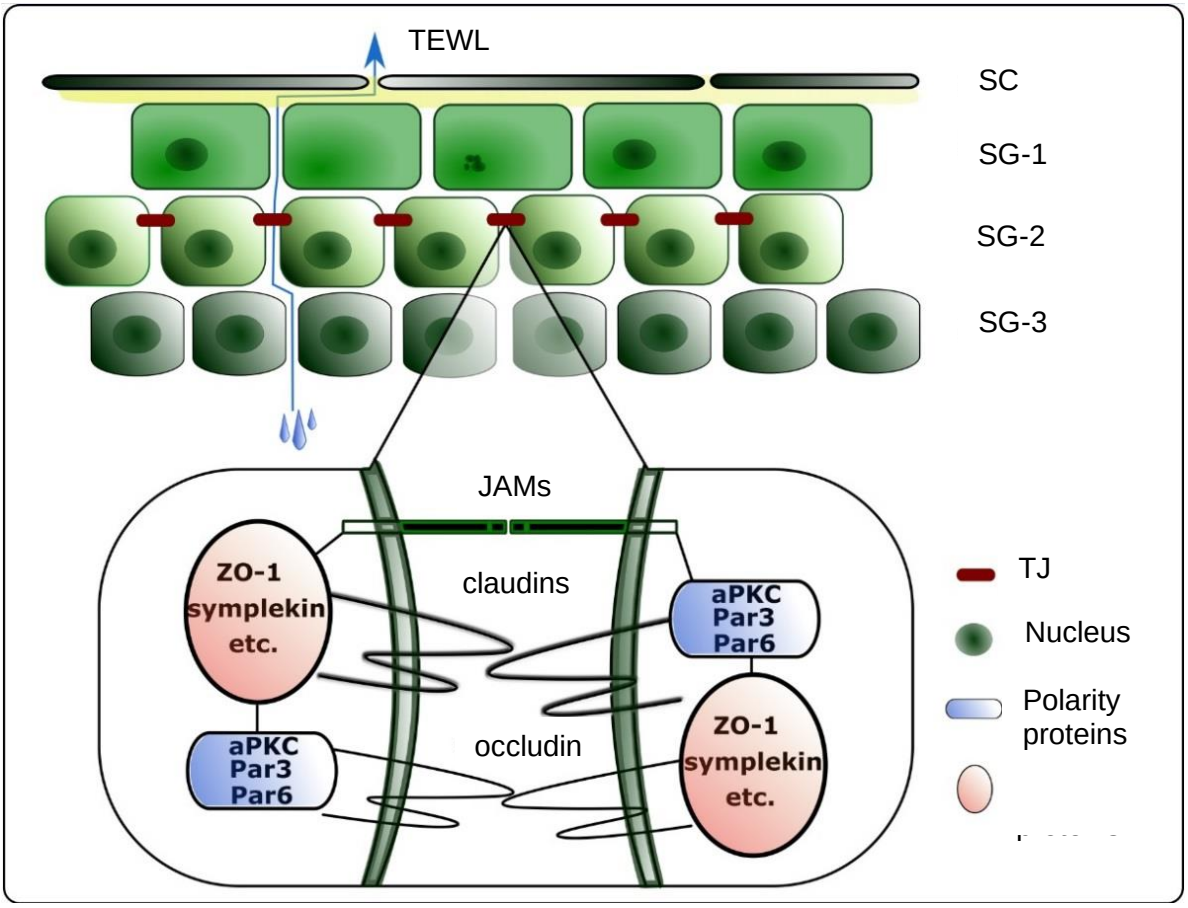

Figure 1: Localization, structure and protein composition of epidermal TJ. *JAM, junctional adhesion molecules; Par, partitioning defective; aPKC, atypical protein kinase; SC, stratum corneum; SG, stratum granulosum; TEWL, trans epidermal water loss; TJ, tight junction.*

2 Aims of the thesis

This project was focused on setting up methods for analysis of the skin barrier in the process of ageing. First of all, a comprehensive review of the skin barrier topic has been made in order to establish the main hypothesis and list of objectives, which resulted in a published paper. The main hypothesis of this thesis challenges the TJs and their potential capability to regulate the barrier function of the aged skin. Since epidermal TJs, epidermal lipids and their mutual interplay define the skin barrier, these were the main points of interest for the analysis.

One of the first objectives was to narrow down the selection of TJ proteins by analyzing TJ expression differences between young and aged skin samples. Next important objective was to implement a suitable skin sampling technique as a substitution for punch biopsy. Two alternatives, SB and TS have been tested for the purpose of future epidermal analyses and their impact on subject safety and well-being. The results have been used for the next published paper. Subsequent objective was focused on an optimization of the RNA/protein co-extraction workflow from the human and porcine epidermis. Optimization of individual methods for the analysis of TJ protein expression followed afterwards, mainly antibodies and workflow for WB and IHC with CLSM. Results of this progress have been orally presented at a conference. In parallel, another objective dealt with a selection of an optimal analytic method for epidermal lipids. Lipid composition of porcine epidermis has been tackled with shotgun MALDI MS technique (presented via poster). However, gold standard HPTLC proved to be more valuable for analysis of epidermal lipids. Next objective dealt with analysis of the aged human skin barrier. Study design had to be approved be by ethics committee to perform skin sampling and non-invasive measurement on human volunteers. Established analytic methods were used to compare the state of young and aged skin barrier and to pinpoint potential TJ protein targets.

The last objective was to mimic the state of aged skin barrier with decreased content of barrier lipids due to years of sunlight exposure by developing a delipidated porcine ex vivo model. Because occludin as a key member of TJ proteins was found to be upregulated in the aged skin and also as a response to the acute skin barrier damage, we evaluated whether its overexpression could improve the water barrier in our ex vivo delipidated skin model as well. For this purpose, a NPWDQ casein-derived peptide previously described as a specific occludin stimulator in epithelial cells (Tanabe 2012) was synthesized and characterized for the induction of occludin overexpression in the delipidated porcine model.

3 Materials and methods

3.1 Suction blistering and tape-stripping characterization

3.1.1 Donors

20 healthy volunteers were recruited for this study. The volunteers gave written informed consent for epidermal sampling by either SB or TS technique. The group of 10 volunteers for SB consisted of 3 males and 7 females with age average 45 years, range 20-74 years. The group of 10 volunteers for TS consisted of 1 male and 9 females with age average 30 years, range 23-44 years. This study was approved by the Ethical Committee of Contipro a.s. according to WMA Helsinki Declaration.

3.1.2 *In vivo* skin imaging

In vivo RCM imaging was performed on the sampling sites of all volunteers prior to TS and post TS using Vivascope 1500 (Mavig, Munich, Germany). 36 x 3.26 μm stacks were taken from a single spot covering total depth of 114 μm. The same settings were utilized for each imaging.

3.1.3 Epidermal sampling and extraction

SB was performed on the left volar forearm of the donors by one person, an acknowledged and well-trained medical laboratory technician. A home-modified syringe with an inner diameter of 0.9 cm was utilized to form the blister as described elsewhere (Gupta et al. 1999). Briefly, the syringe was connected to a vacuum pump with a CVC 3000 vacuum controller (Vacuubrand, Essex, CT, USA) through a two-way valve. Once a negative pressure of 250 mmHg was developed, the two-way valve was sealed. After the blister formation, the blister fluid was discarded and the blister roof (the epidermis) collected. Each epidermal sample was divided into three parts, one half and two quarters. The half of the sample was used for protein and RNA extraction and the two quarters were used for IHC and lipid analyses, respectively.

TS was also performed on the left volar forearm of the volunteers by one person, an acknowledged medical laboratory technician. 30 D-Squame discs (diameter 1.4 cm, CuDerm, Dallas, TX, USA) were consecutively applied onto the same spot and removed. The obtained material by both techniques was weighed using analytical scales. For the weighing of the TS samples TS discs were pooled by ten (strip number 1-10, 11-20, 21-30).

The obtained material was homogenized in RNAzol® RT (MRC, Cincinnati, OH, USA) reagent either by TissueLyser II (QiaGen, Hilden, Germany) with RNAse free stainless-steel beads in case of SB samples or by vigorous shaking for 30 minutes in case of TS. Total RNA and protein isolation were performed according to the manufacturer's protocol with some modifications to maximize the yield. Briefly, diethylpyrocarbonate-treated water was added to RNAzol® sample lysate and the mixture was vigorously shaken for 15 seconds and stored for 15 minutes at RT. Samples were centrifuged 12,600 g for 15 minutes at 8°C and a water phase containing RNA was collected. The RNA isolation continued by the column extraction protocol on a Qiacube automated isolator

(QiaGen, Hilden, Germany). The protein isolation continued by washing the residual pellet twice with 75% ethanol. The pellet was then dissolved using a lysis buffer (4 M urea, 150 mM NaCl, 50 mM Tris, 1 % Triton-X, 1 % SDS). After centrifugation (13,500 g, 15 minutes) the supernatant was collected. Protein and RNA isolates were stored at -80°C until further analysis.

3.1.4 SDS-PAGE and western blotting

Protein concentrations in the protein isolates were assessed by Pierce™ BCA Protein Assay Kit (ThermoFischer Scientific, Waltham, MA, USA). Isolated protein amounts (7 μg for the TS samples and 35 μg for the SB samples) were loaded onto 12% polyacrylamide gel and after the separation, the proteins were transferred to an Immuno-Blot® PVDF membrane (Bio-Rad, Hercules, CA, USA). After blocking for 60 minutes with 5% skim milk in TBS-T, the membranes were incubated with the primary antibodies against claudin-1 (clone 2H10D10, 1:500, cat.no. 37-4900), occludin (clone OC-3F10, 1:300, cat.no. 33-1500), ZO-2 (polyclonal, 1:200, cat.no. 71-1400), filaggrin (mouse monoclonal FLG01, 1:500, cat.no. MA5-13440) (all ThermoFischer Scientific, Waltham, MA, USA), laminin (rabbit polyclonal, Abcam, Cambridge, UK, 1:500, ab11575) and GAPDH (rabbit polyclonal, Sigma-Aldrich, St.Louis, MO, USA, 1:1000, cat.no. G8795) overnight at 4°C. After a subsequent washing in TBS-T, the membranes were incubated for 60 minutes with the respective secondary antibodies conjugated with HRP (anti-rabbit IgG-HRP antibody produced in goat, anti-mouse IgG-HRP produced in rabbit, both Sigma-Aldrich, St.Louis, MO, USA, 1:1000, cat.no. A0545 and A9044). After a subsequent washing with TBS-T, the protein-antibody complexes were visualized with the SuperSignal™ West Pico Chemiluminescence Substrate (ThermoFischer Scientific, Waltham, MA, USA) and detected by an Alliance 4.7 chemiluminescence detector (UVItec Limited, Cambridge, UK).

3.1.5 RNA amplification and quantitative real-time RT-PCR

The concentration and purity of isolated RNA were determined by a Cary50 UV-VIS spectrophotometer (Agilent Technologies, Santa Clara, CA, USA) using the 260/280 absorption ratio. A reverse transcription reaction was performed with 1 μg of isolated RNA using High Capacity RNA-to-cDNA Kit (ThermoFischer Scientific, Waltham, MA, USA) as suggested by the manufacturer. Subsequent qPCR was performed with TaqMan gene expression assays for *FLG* (Hs00856927_g1), *OCLN* (Hs00170162_m1), *CLDN1* (Hs00221623_m1), *LAMA3* (Hs00165042_m1) and *RPL13A* (Hs04194366_g1) genes. For TS samples with low initial concentration of RNA (below 30 $ng.\mu L^{-1}$) we used RNA amplification kit Ovation PicoSL WTA System V2 (NuGen, Manchester, UK) according to the manufacture's manual. After the amplification, we purified the samples on the Agencourt magnetic beads (BeckmanCoulter, Brea, CA, USA) as recommended. Finally, we determined the concentration and purity of the amplified RNA samples, which were then used for the quantitative real-time reverse transcription PCR (qRT-PCR) as described above.

3.1.6 Immunohistochemistry

One fourth of the collected epidermis from SB was frozen in an optimal cutting temperature compound Cryomount (Histolab, Göteborg, Sweden) and stored at -80°C

until further use. Cross-sections (7 μm) were obtained by a Leica CM1950 cryostat (Leica Biosystems, Wetzlar, Germany) and fixed in acetone at -20°C for 10 minutes. For the TS samples the 30th TS disc was chosen for the IHC staining. The TS disc was fixed in 4% paraformaldehyde solution for 10 minutes at RT and permeabilized with use of 0.2% solution of Triton X-100 in TBS for 15 minutes. The sections and the TS disc were then blocked by 5% BSA in 0.1% TBS-T solution for 60 minutes at RT and probed with primary antibody against claudin-1 (clone 2H10D10, 1:200, cat.no. 37-4900) for 60 minutes at RT. After washing with TBS-T, the sections and the TS disc were incubated with the appropriate secondary antibody conjugated with Alexa 647 (1:200, cat.no. A-21235) (both ThermoFischer Scientific, Waltham, MA, USA) for 60 minutes at RT. After subsequent washing with TBS-T, the sections and the TS disc were mounted in a Prolong Diamond medium with 4′,6-diamidino-2-phenylindole (DAPI) (ThermoFischer Scientific, Waltham, MA, USA). Images were acquired by a Leica TCS SP8 X confocal laser scanning microscope (Leica Microsystems, Wetzlar, Germany) using a HyVolution mode and deconvoluted by HuygensEssential software (Scientific Volume Imaging, Hilversum, Netherlands).

3.1.7 Lipid analysis

IR spectra of the SB epidermal samples were collected on a Nicolet 6700 FT-IR spectrometer (Thermo Fisher Scientific, Waltham, USA) equipped with a single-reflection MIRacle attenuated total reflectance germanium crystal at 23°C. The spectra were generated by a co-addition of 256 scans collected at 4 cm-1 resolution and analyzed with Bruker OPUS software. The exact peak positions were determined from the second derivative spectra and by a peak fitting if needed.

For the extraction of the epidermal lipids, a modified Bligh and Dyer method was used (Bligh and Dyer 1959). The epidermal samples were extracted with 1 mL chloroform/methanol ($CHCl_3$/MeOH) 2:1 (v/v) per mg of the epidermis for 90 minutes, filtered, separated and concentrated under a stream of nitrogen. The lipids were dried and stored at -20°C under argon. The lipids were analyzed on silica gel 60 HPTLC plates (20 × 10 cm, Merck, Darmstadt, Germany). The extracted epidermal lipids were dissolved in 100 μl CHCl3/MeOH 2:1. 10 - 30 μL of each lipid sample was sprayed on the plate using a Linomat IV (Camag, Muttenz, Switzerland). Standards for the HPTLC analysis (ceramide NS, AS, NP and AP), glucosylceramide and sphingomyelin were purchased from Avanti Polar Lipids (Alabaster, AL, USA) or synthesized (ceramide NH (Kováčik et al. 2016), EOS, EOP and EOH (Opálka et al. 2015)). Cholesterol, cholesteryl sulfate, fatty acid standards, L-α-phosphatidylcholine and all other agents were purchased from Sigma-Aldrich (Schnelldorf, Germany) if not otherwise stated. Standard lipids were dissolved in $CHCl_3$/MeOH 2:1 (v/v) (ceramides, cholesterol and free fatty acids), and $CHCl_3$/MeOH 1:1 (v/v) (cholesteryl sulfate, glucosylceramide, sphingomyelin and L-α-phosphatidylcholine), respectively, at 1 mg.mL-1. To generate calibration curves, the lipids were mixed in ratios that approximately corresponds to the composition of the human skin (Zoschke et al. 2016). The calibration samples were applied on a HPTLC plate together with the analyzed samples. The major skin barrier lipids (ceramides, free fatty acids and cholesterol) were separated using $CHCl_3$/MeOH/acetic acid 190:9:1.5 (v/v/v) mobile phase twice to the top of the plate (Bleck et al. 1999; Vávrová et al. 2014). The ceramide precursors (glucosylceramide

and sphingomyelin), phospholipids and cholesteryl sulfate were separated using a more polar mobile phase ($CHCl_3$/MeOH/acetic acid/H_2O 65:25:6:3) (Vávrová et al. 2014; Wallmeyer et al. 2015). The lipids were visualized by dipping in a derivatization reagent (7.5% $CuSO_4$, 8% H_3PO_4, 10% MeOH in water) for 10 seconds and heating at 160°C for 30 minutes and quantitated by densitometry using a TLC scanner 3 and WinCats software (Camag, Muttenz, Switzerland).

3.2 Skin barrier and tight junctions analysis

3.2.1 Demography of human donors

The study design was approved by the Ethical Committee of Contipro a.s. according to WMA Helsinki Declaration. 20 healthy Caucasian volunteers were recruited and assigned into two groups according to age, young (median 17 years, range 16-21 years; female/male 11/1, n=12) and aged (median 68 years, range 52-84 years; female/male=4/4 n=8). The volunteers or legally acceptable representatives (in case of youths) gave written informed consent for the participation in this study. The volunteers did not suffer from any skin disease or any other serious systematic disease such as diabetes mellitus and were not using any medicaments. The sampling was conducted during June before the main summer season and all the volunteers had avoided extensive sunlight exposure 14 days prior to the skin sampling.

3.2.2 Non-invasive *in vivo* biophysical skin analysis

Prior to SB, both skin sites, sun-protected (volar) and sun-exposed (dorsal), of each volunteer's forearm were probed by a Tewameter® TM300 probe (Courage + Khazaka electronic, Cologne, Germany) and by a Vivascope reflectance confocal microscope (Mavig, Munich, Germany) after 30 minutes of acclimation. The same settings were utilized for each imaging.

3.2.3 Microarray analysis

TS samples of the epidermis of young (18 ± 1 years, n=4) and aged (57 ± 2 years, n=4) donors were collected from sun-protected lower part of back neck. RNA was isolated from twenty TS discs (RNeasy Micro Kit, Qiagen, Hilden, Germany), amplified (Ovation® RNA Amplification System V2, NuGEN, USA), fluorescently-labeled (WGA2 - GenomePlex® Complete Whole Genome Amplification (WGA) Kit, Sigma-Aldrich, St.Louis, MO, USA) and hybridized to a microarray (Human Gene Expression 4x44K v2 chip, Agilent Technologies, Santa Clara, CA, USA). Data were analyzed with software R (R Development Team) and differential gene expression was determined between the two age groups using R statistical package limma.

3.2.4 Epidermal sampling and extraction

After the non-invasive skin analysis, SB was performed on sun-protected (volar) and sun-exposed (dorsal) skin sites of the left forearm of the volunteers by one person, an acknowledged medical laboratory technician. A modified syringe with an inner diameter of 0.9 cm was utilized to form the blister as described elsewhere (Svoboda et al. 2017).

Briefly, the syringe was connected to a vacuum pump with a CVC 3000 vacuum controller (Vacuubrand, Essex, CT, USA) through a two-way valve. Once a negative pressure of 250 mmHg was developed, the two-way valve was sealed. The blister fluid was discarded and the blister roof (the epidermis) collected. The samples of collected epidermis were divided into three parts, i.e., one half and two quarters. The half of the sample was used for the protein and RNA extraction and the two quarters were used for IHC and lipid analysis.

The obtained material was homogenized in RNAzol® RT (MRC, Cincinnati, OH, USA) reagent by a TissueLyser II homogenizer (Qiagen, Hilden, Germany) with RNAse free stainless-steel beads. The total RNA and protein isolation as described in chapter 3.2.4. with little adjustments. Briefly, diethylpyrocarbonate-treated water was added to a RNAzol® sample lysate and the mixture was vortexed for 20 seconds and stored for 20 minutes at RT. Protocol then continued as in 3.2.4.

3.2.5 Quantitative real-time RT PCR

The concentration and purity of isolated RNA were determined by a Cary50 UV-VIS spectrophotometer (Agilent Technologies, Santa Clara, CA, USA) using the 260/280 absorption ratio. A reverse transcription reaction was performed with 1 μg of isolated RNA using the High Capacity RNA-to-cDNA Kit (ThermoFischer Scientific, Waltham, MA, USA) as suggested by the manufacturer. Subsequent qPCR was performed with TaqMan gene expression assays (ThermoFischer Scientific, Waltham, MA, USA) for *CLDN1* (Hs00221623_m1), *OCLN* (Hs00170162_m1), *TJP2* (Hs00910543_m1) and *RPL13A* (Hs04194366_g1) genes in case of the human epidermis, and for *OCLN* (Ss03377507) and *RPL13A* (Ss003376908_u1) in case of the porcine epidermis. The threshold cycle was determined for the genes of interest and the relative mRNA level in each sample was calculated using the $2^{-\Delta\Delta CT}$ method (Livak and Schmittgen 2001).

3.2.6 SDS-PAGE and western blotting

Same protocol was performed as described in chapter 3.2.5. only that the membranes were incubated with the primary antibodies against claudin-1 (clone 2H10D10, 1:500, cat.no. 37-4900), occludin (clone OC-3F10, 1:300, cat.no. 33-1500), ZO-2 (polyclonal, 1:200, cat.no. 71-1400) (ThermoFischer Scientific, Waltham, MA, USA) and GAPDH (polyclonal, Sigma-Aldrich, St.Louis, MO, USA, 1:1000, cat.no. G8795) overnight at 4°C.

3.2.7 Immunohistochemistry and confocal microscopy

Tissue samples were frozen in a Cryomount optimal cutting temperature compound (Histolab, Göteborg, Sweden) and stored at -80°C until further use. Cross-sections (7 μm) were obtained by a Leica CM1950 cryostat (Leica Biosystems, Wetzlar, Germany) and fixed in acetone at -20°C for 10 minutes. The sections were then blocked by 5% BSA in 0.1% TBS-T solution for 60 minutes at RT and probed with the primary antibodies against claudin-1 for 90 minutes (clone 2H10D10, 1:200, cat.no. 37-4900), occludin for 30 minutes (clone OC-3F10, 1:100, cat.no. 33-1500) or ZO-2 for 60 minutes (polyclonal, 1:200, cat.no. 71-1400) at RT. After washing with TBS-T, the sections were incubated with the appropriate secondary antibody conjugated with Alexa 647 (1:500, cat.no. A-21235) or Alexa 488 (1:500, cat.no. A-11008) for 60 minutes at

RT. After subsequent washing with TBS-T, the sections were mounted in Prolong Diamond with DAPI (all ThermoFischer Scientific, Waltham, MA, USA). Images were acquired by a Leica TCS SP8 X confocal laser scanning microscope (Leica Microsystems, Wetzlar, Germany). Representative images were obtained using HyVolution mode and deconvoluted by HuygensEssential software (Scientific Volume Imaging, Hilversum, Netherlands). For quantification purpose, images were acquired using the Leica Hybrid Detector Photon Counter along with the white light laser and retaining the same settings for each image. A stack of 7.2 µm was acquired for each cross-section and the fluorescent signal was quantified in the whole stack.

3.2.8 Lipid analysis

For lipid analysis, please see chapter 3.2.8 and 3.2.9.

3.2.9 Skin barrier disruption model

Fresh porcine auricles were purchased from a local slaughterhouse and immediately used for the experiments. After the auricle was cleansed, samples (5 x 5 cm) of the full-thickness skin were obtained from the inner side of the auricle. The samples were disinfected and incubated in 2.4 U mL^{-1} Gibco® Dispase II (Thermo Fisher Scientific, Waltham, USA) solution over night at 4°C in a Petri dish with a dermal side facing the bottom of the dish while the epidermis was exposed to air. Epidermal samples were obtained after 18 hours, washed in a sterile PBS solution and inserted into modified Franz diffusion cells containing a porous polyamide membrane and a culture medium. The culture medium consisted of a MCDB 153 medium with 0.3 mg mL^{-1} adenine, 4.9 ng mL-1 apo-transferrin, 1.4 ng mL-1 triiodo-L-thyronine, 0.8 µg mL^{-1} hydrocortisone, 10 ng mL^{-1} insulin, 2 ng mL^{-1} cholera toxin, 2 ng mL^{-1} hEGF and supplemented with penicillin, streptomycin and amphotericin B. The resultant ex vivo porcine epidermis was cultured at “air-liquid interface” with 5% CO2 at 37°C for the next 6 days.

A casein-derived peptide NPWDQ was synthetized following standard Fmoc/HBTU/DIPEA protocols using 2-chlorotrityl resin (Agilent Technologies, Santa Clara, CA). Fmoc-amino acids and chemicals used in the synthesis and cleavage were obtained from Iris Biotech GmbH (Marktredwitz, Germany). The crude peptide was precipitated with diethylether and purified. The purity was confirmed by LC-MS 2020 (Shimadzu Europa, Duisburg, Germany) using a Jupiter® Proteo 90 Å reverse phase column (Phenomenex, Torrance, CA).

Ex vivo porcine epidermis specimens were placed into the modified Franz cells as described above and cultivated at 37°C, 5% CO_2 in a humidified atmosphere for 24 hours. Subsequently, initial TEWL values of the ex vivo porcine epidermis were measured by a Tewameter® TM300 probe (Courage + Khazaka electronic, Cologne, Germany). After the TEWL measurement, the ex vivo porcine epidermis was delipidated using acetone as described elsewhere to yield an epidermal model with the delipidated SC (Rissmann et al. 2009). Briefly, acetone-soaked cotton swabs were moved back and forth over the surface of the model. Afterwards, a surface of the delipidated epidermal model was rinsed with a sterile PBS solution. TEWL rates of the delipidated epidermal model were measured 24 hours after the delipidation. Subsequently, the ex vivo porcine epidermis was treated with 1.6 x 10-4 M NPWDQ

peptide in the culture medium or control (culture medium), which were placed in both the donor and acceptor chambers of Franz diffusion cells. Another TEWL rates were measured 48 and 120 hours after the delipidation. The Franz diffusion cells were then dismantled, and the ex vivo porcine epidermis retrieved for the total RNA isolation and IHC analysis by the aforementioned protocols.

3.2.10 Statistical analysis

Data analysis was performed using Prism 7 software (GraphPad Software, San Diego, CA, USA). Data are presented as means ± SEM. Normality of the data was checked by D'Agostino-Pearson normality test and statistical significance was calculated using paired or unpaired t-test. $P < 0.05$ was considered significant.

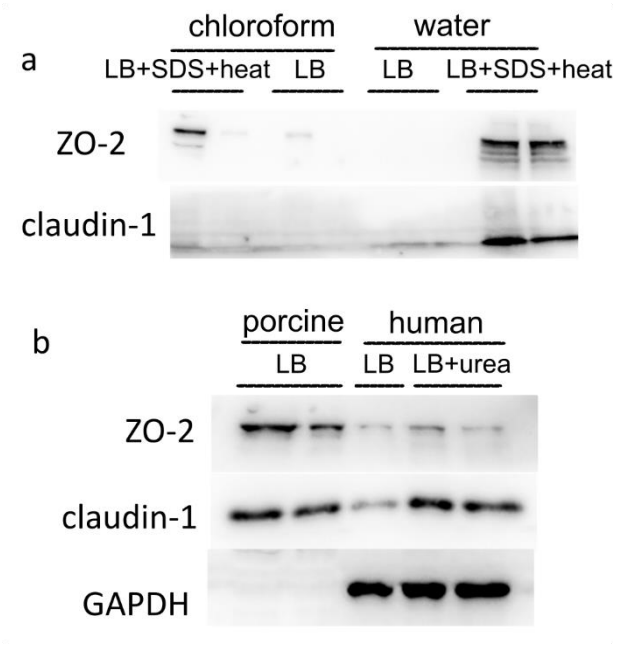

Figure 2: Optimization of a protein extraction from the epidermis samples. *(a) Different extraction procedures from porcine epidermis samples based either on chloroform or water. (b) Effect of enhanced lysis buffer (LB) on the extraction of either porcine or human epidermis.*

4 Results

4.1 Methods Optimization

Enhanced manufacturer's protocol procedure for extracting RNA and proteins from the porcine or human epidermis worked the best – both adding SDS/heat and urea improved yield of ZO-2, claudin-1 and GAPDH, see Figure 2. Chloroform based coextraction of RNA and proteins showed very low yields of proteins in comparison to water based coextraction. Anti-GAPDH antibody was shown to be inappropriate for the porcine epidermis

The ideal set up for the claudin-1 detection was dilution of primary antibody (2H10D10) 1:200 incubated for 90 minutes at RT. No difference in the staining was observed when using human or porcine skin (data not shown). The ideal set up for occludin was dilution of primary antibody (OC-3F10) 1:100 incubated for 30 minutes at RT. Anti-occludin worked on the human skin specimens with no problem. But, in the porcine skin occludin was detectable only with OC-3F10. Other anti-occludin antibodies were not efficient in detection of occludin in the porcine skin (data presented in (Svoboda 2020)). Ideal ZO-2 set up included dilution of primary antibody 1:100 for 60 minutes at RT (data not shown).

4.2 Suction blistering and tape-stripping characterization

Sampling durations of both techniques were roughly comparable (SB average 62 minutes, range 39-105 minutes; TS average 50 minutes, range 47-55 minutes). According to the subjective evaluation, both SB and TS were equally painful, more precisely, little or no pain was reported by the volunteers. The skin of some volunteers developed a slight local hyperpigmentation after SB as well as TS procedure. The hyperpigmentation lasted for less than month in case of TS and over a six month in case of SB (data presented in (Svoboda 2020) or (Svoboda et al. 2017)). Both techniques left no permanent damage.

The SB samples provided more biological material than the TS samples (Figure 3a) even though TS covered a larger area, 1.54 cm2, than the SB samples, which ranged from 0.2 cm2 to 0.5 cm2. Results also showed that significantly less material is obtained towards the living part of the epidermis by TS. The yield of the protein and RNA was disproportionally higher in SB than in TS regarding the weight of biological material obtained, suggesting that the extraction of the TS samples was not very effective (Figure 3b and 3c).

All genes analyzed by qRT-PCR were detected in the SB samples, presented in (Svoboda 2020; Svoboda et al. 2017). However, only FLG and RPL13A were successfully detected in the TS samples since OCLN, CLDN1 and LAMA3 remained undetermined. A similar trend was observed on a protein level as well. The WB analysis showed that all the analyzed proteins are detectable in the SB samples, whereas only GAPDH and filaggrin were detected in the TS samples, presented in (Svoboda et al. 2017). This suggests that 30 consecutive TS discs were sufficient to reach the SG but were not effective to detach it. RCM imaging showed characteristic structures of the

human epidermis before and after TS and confirms the fact that TS did not detach the SG layer (Figure 4).

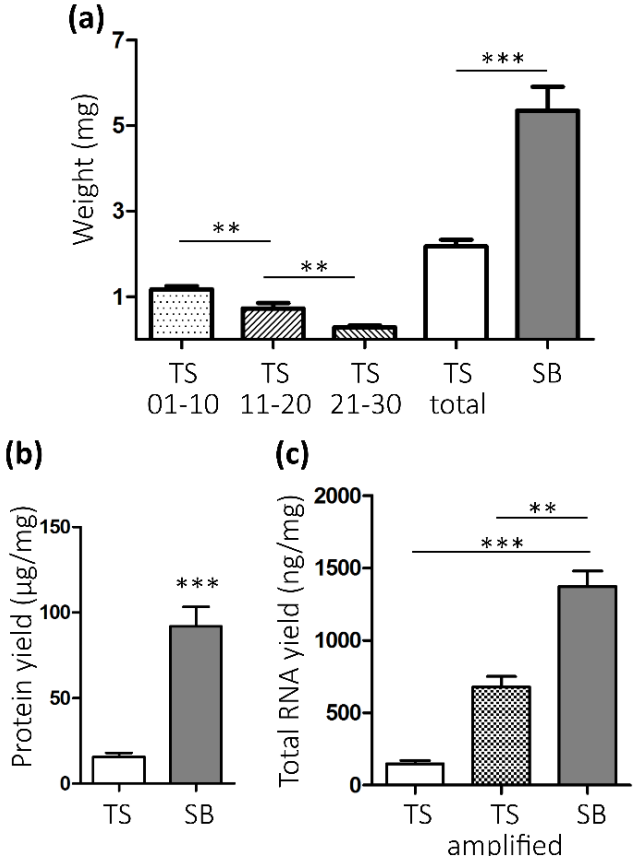

Figure 3: Comparison of the RNA and protein yields of the TS and SB sampling techniques*. Weight of the obtained material from 30 consecutive strips (TS) and SB from volar forearm of 10 volunteers for each technique (a). Protein yield per mg of obtained material (b). Total RNA yield per mg of obtained material (c). The data represent mean ± SEM; **P<.01; ***P<.0001*

The epidermal structure seemed to be intact and the expression pattern of claudin-1 in the SB samples is congruent with the literature (Figure 5), while in the TS samples a very faint fluorescent signal occurs that cannot be considered as a specific signal of claudin-1. Also, no signal for cell nuclei is present in the TS samples as expected, only clusters of corneocytes are visible within a transmission detector channel (Figure 5).

IR spectroscopy of the SB samples (one quarter of the blister collected) showed the presence of highly ordered SC lipids (as indicated by methylene stretching wavenumbers) and the co-existence of a very tight orthorhombic chain with slightly looser hexagonal lipid packing. HPTLC analysis showed the presence of all barrier lipids in correct proportions (8 ceramide subclasses, FFA, cholesterol and cholesteryl sulfate) and their precursors (SM, glucosylceramides and phospholipids (PL)). However, PL class was notably decreased. Figures shown in (Svoboda et al. 2017).

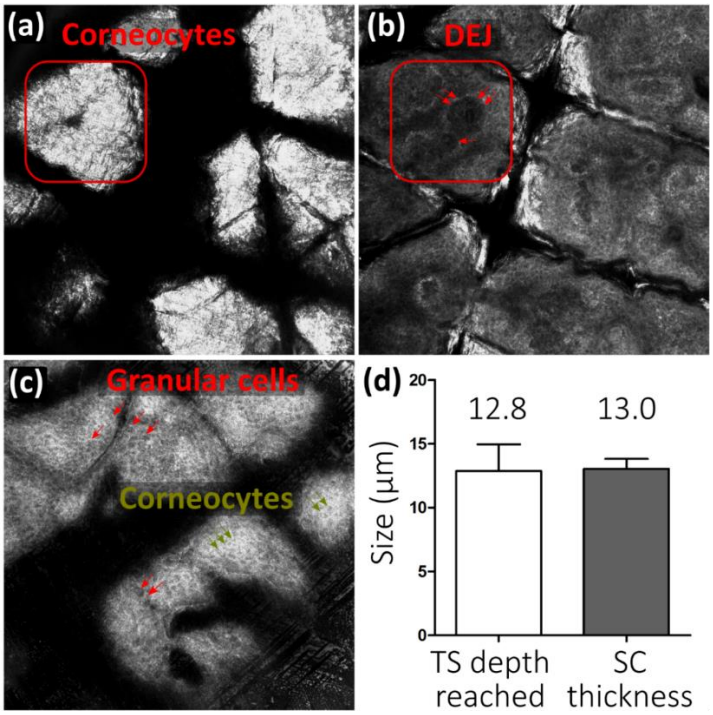

Figure 4: RCM imaging of the tape-stripped skin*. The uppermost image prior to TS indicating undamaged SC with clusters of corneocytes (a). Image indicating start of the dermo-epidermal junction (DEJ) which is the endpoint for thickness measurement (b). The uppermost image after TS indicating presence of the SG (honeycomb pattern) with granular cells (red arrows) and residual corneocytes (green arrows) (c). Size comparison of the depth reached by TS and SC thickness in 10 healthy volunteers (d). RCM image = 0.5 x 0.5 mm. The data represent mean ± SEM. DEJ, dermo-epidermal junction.*

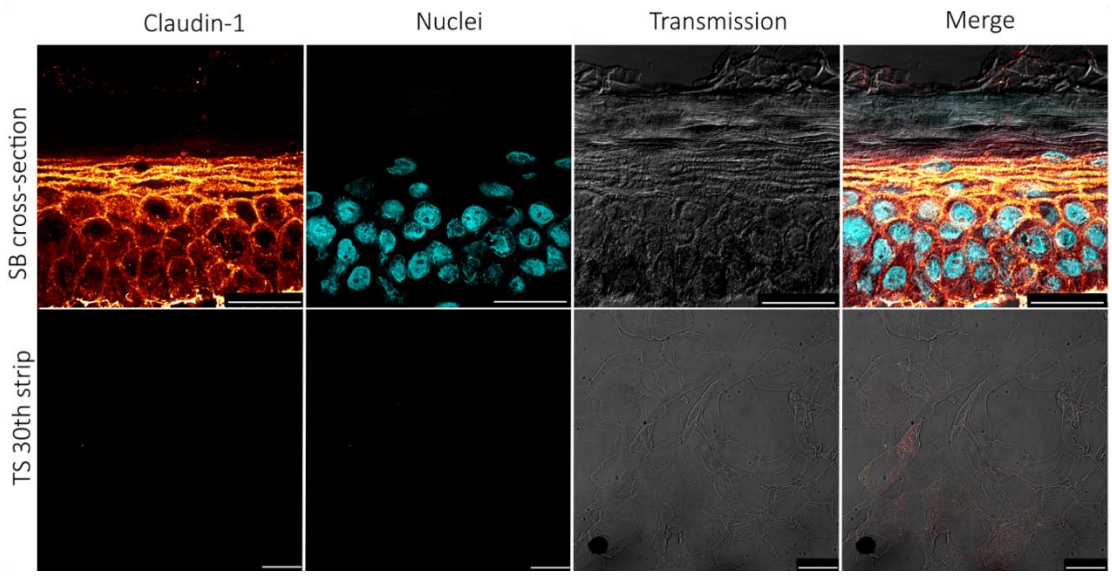

Figure 5: Representative IHC staining *of a SB cross-section and the 30th TS disc both acquired from left volar forearm. Images of merged channels show the localization of claudin-1 (orange), cell nuclei (teal) and epidermal structure by transmission detector. Bar = 25 µm.*

4.3 Skin barrier and tight junctions analysis in the sun-protected and sun-exposed, young and aged human epidermis

To assess the condition of the skin barrier we analyzed the lipid composition and organization and TEWL in the sun-protected and sun-exposed forearm skin of aged and young donors. TEWL showed no differences either between the young and aged or between the sun-protected and sun-exposed skin (Figure 6a). Furthermore, a structure of the young and aged epidermis was analyzed in vivo by the reflectance confocal microscopy. Apart from an increased melanin content in melanocytes and basal keratinocytes in the sun-exposed area, we noticed fewer structures corresponding to rete pegs at dermo-epidermal junctions in the aged skin, presented in (Svoboda 2020).

The HPTLC analysis showed 15% lesser amount of the total barrier lipids in the aged sun-exposed skin than in the young sun-exposed skin and aged sun-protected skin (Figure 6b), which is congruent with lipid/protein ratio. The lesser amount of total barrier lipids in the aged sun-exposed skin is reflected by a lowered amount of free fatty acids and cholesterol (Figure 6d). In contrast, total ceramides as the main constituents of the lipid barrier (Coderch et al. 2003) did not differ between the studied groups (Figure 6d). Furthermore, detailed ceramide analysis did not reveal any significant changes in ceramide subclasses, presented in (Svoboda 2020) . Interestingly, the young sun-protected skin had fewer barrier lipids than the aged sun-protected or young sun-exposed skin (Figure 6b).

Complementary information from IR shows that young sun-exposed skin is less ordered than young sun-protected, and that the broader lipid chain order can be found in aged sun-exposed when compared to young sun-exposed, presented in (Svoboda 2020).

4.3.1 Occludin expression is elevated in the human photoaged skin and ZO-2 expression is increased in the sun-exposed and sun-protected aged skin

Claudin-1, occludin and ZO-2 selection was based on a microarray analysis and previously described roles of TJ proteins in the skin barrier, presented in (Svoboda 2020). Claudin-1-/- mice exerted lethal TEWL after birth (Furuse et al. 2002), the occludin overexpression was present in the recovering epidermal barrier (Malminen et al. 2003; Yamamoto et al. 2008), and the ZO-2 knockdown deteriorated barrier function (Roy et al. 2014). Next, we determined the expression of claudin-1, occludin and ZO-2 on the mRNA as well as protein level. The expression of CLDN1/claudin-1 on the mRNA and protein levels was not consistent. Although CLDN1 mRNA was expressed significantly more in the aged sun-exposed skin in comparison to other groups (Figure 7a), the expression of claudin-1 on the protein level was significantly increased in the young sun-protected area as analyzed by WB (Figure 7b). A similar trend of the claudin-1 expression on the protein level was acquired by IHC (Figure 7c and 8), although with no statistical significance.

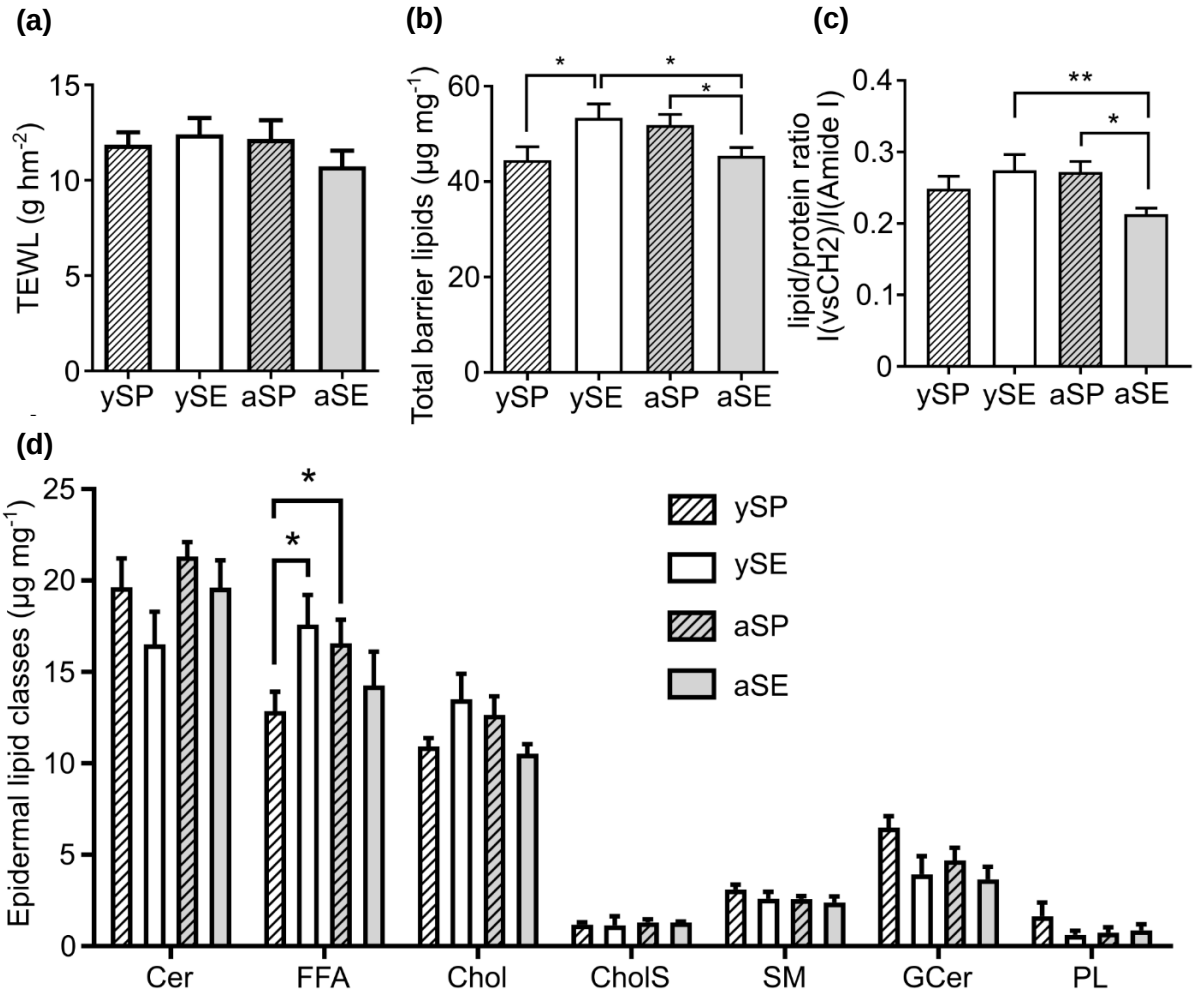

Figure 6: Condition of the young and aged skin barrier in sun-exposed and sun-protected skin of human donors as indicated by TEWL and lipid analysis*. (a) TEWL rates measured in vivo by an open-chamber method prior to the suction blister sampling. (b) Total epidermal lipids in suction blister samples quantified by densitometry after HPTLC separation. (c) The lipid/protein ratio in suction blister samples evaluated by IR spectroscopy as a ratio of intensities of methylene symmetric stretching vibration that originates mostly from lipids and Amide I band that originates mostly from the peptide bond. (d) Composition of barrier lipids (Cer, FFA, Chol) and their precursors (GCer, SM, CholS, PL) in the suction blister samples quantified by densitometry after HPTLC separation. The data are shown as mean ± SEM (young n=12, aged n=8). Statistical significance * P < 0.05, ** P < 0.01. aSE, aged sun-exposed; aSP, aged sun-protected; CholS, cholesterol sulfate; FFA, free fatty acids; GCer, glucosylceramide; PL, phospholipid; SM, sphingomyelin; TEWL, transepidermal water loss; ySE, young sun-exposed; ySP, young sun-protected.*

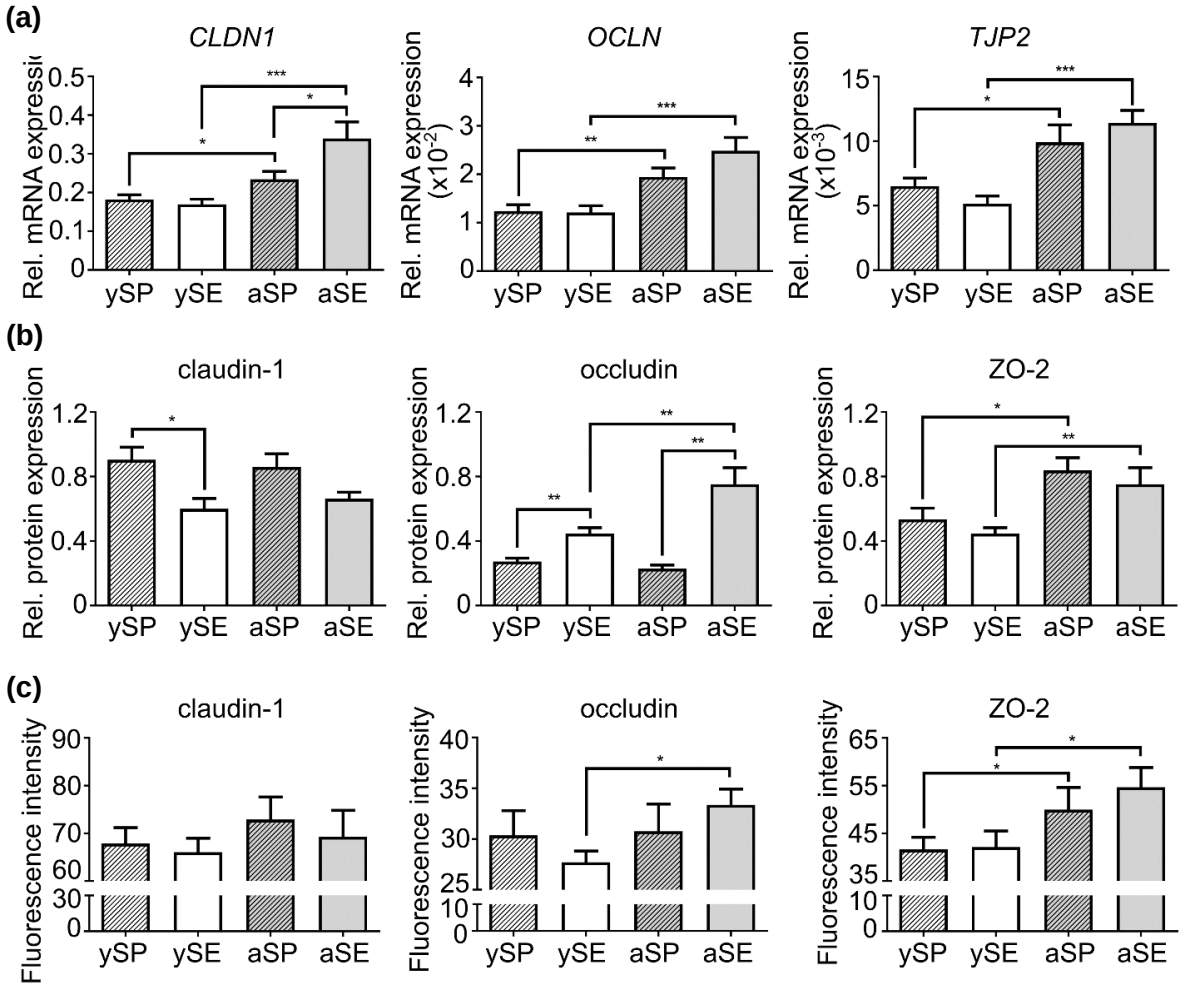

Figure 7: Expression of claudin-1, occludin and ZO-2 in the sun-exposed and sun-protected epidermis of young and aged human forearm skin on the mRNA and protein level. *Samples of human epidermis were acquired by suction blistering from healthy volunteers. (a) Relative expression of CLDN1, OCLN and TJP2 assessed by qRT-PCR. (b) Relative expression of claudin-1, occludin and ZO-2 on the protein level assessed by western blotting. (c) Quantification of fluorescence intensities of claudin-1, occludin and ZO-2 expression from 7.2 µm stacks from histological cross-sections using the Leica Hybrid Detector Photon Counter. Data are shown as mean ± SEM (young n=12, aged n=8), statistical significance *P < 0.05, **P < 0.01, ***P < 0.001.*

All methods confirmed that *OCLN*/occludin was expressed significantly more in the aged sun-exposed skin when compared to the young skin (Figure 7). Other significant differences were also observed, although trends were inconsistent. *OCLN* gene expression levels were elevated in the aged skin – both sun-protected and sun-exposed in comparison to their young counterparts (Figure 7a). On the protein level, WB indicated the elevated occludin expression in the young and aged sun-exposed skin (Figure 7b), while IHC confirmed the upregulation of occludin only in the aged sun-exposed skin (Figure 7c and 8). These results suggest that the photoaging affects the occludin expression in the skin.

The TJP2/ZO-2 expression was elevated on the mRNA as well as protein level in the aged skin of both areas, which was confirmed by all the used methods (Figure 7 and 8). Apparently, the intrinsic aging rather than photoaging affects the ZO-2 expression.

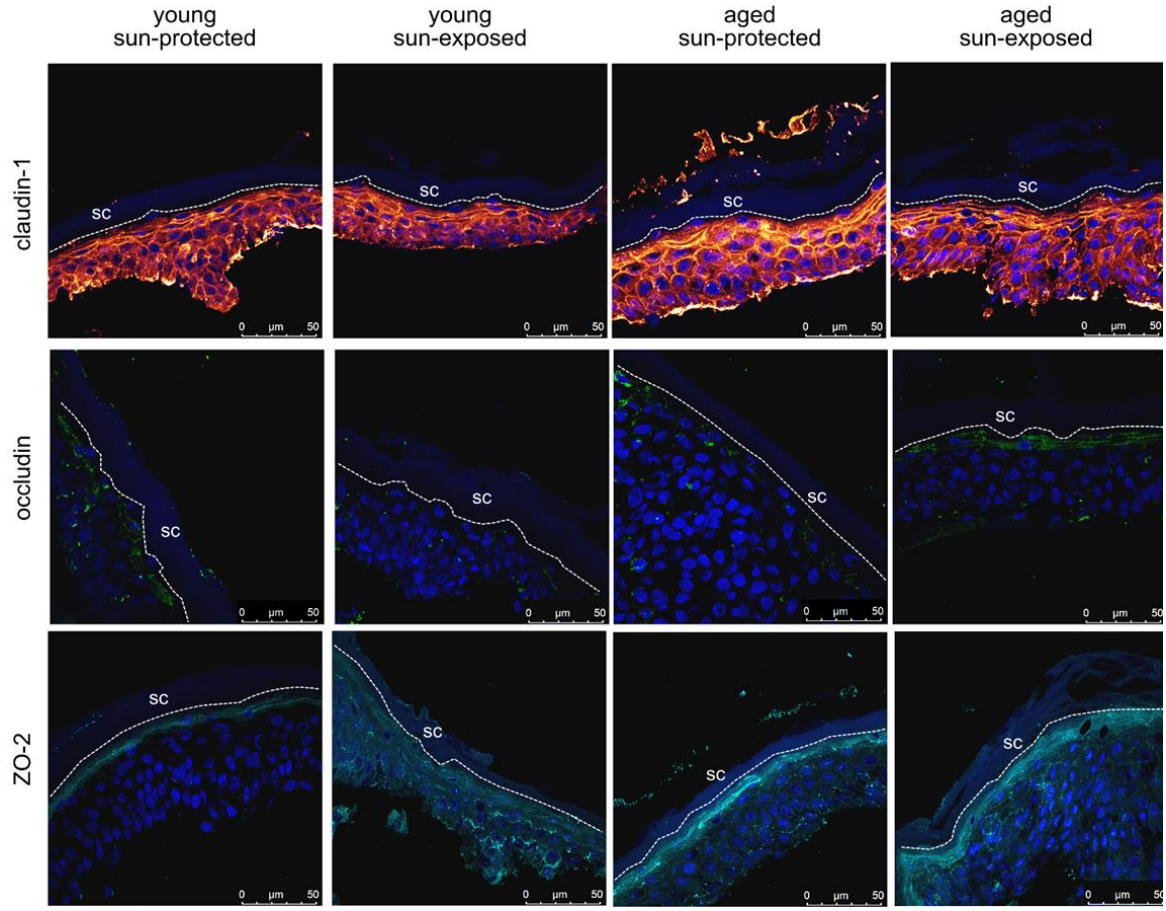

Figure 8: Representative IHC images of claudin-1, occludin and ZO-2 expression in young and aged sun-exposed and sun-protected human forearm skin. *Skin cross-sections were prepared using optimized IHC protocol and visualized with confocal laser scanning microscope. Orange – claudin-1, green – occludin, teal – ZO-2, blue – cell nuclei. Bar=50 µm.*

4.3.2 Occludin overexpression lowers TEWL of *ex vivo* porcine epidermis after delipidation

Since the occludin expression was clearly increased in the photoaged skin where the decreased lipid content was found, we examined the occludin link to the water barrier. To examine whether occludin plays a role in the maintenance of the water barrier in the photoaged skin with decreased lipid content, we used an ex vivo porcine epidermis with delipidated SC as the experimental model. The epidermis was previously shown to re-establish the water barrier after an acute damage. TEWL reached the peak in 3 days, started to decline after 5 days being fully restored within 10 days after the damage (Jiang et al. 2007; Kottner et al. 2013a; Malminen et al. 2003). The ex vivo porcine epidermis exhibited a similar trend after the delipidation with acetone. TEWL doubled 24 hours

after the delipidation and further increased 48 hours after the delipidation. 120 hours after the delipidation, the ex vivo porcine epidermis shows partially recovered TEWL (Figure 9a). To evaluate the potential role of occludin in the re-establishment of the water barrier, we stimulated the occludin expression 24 hours after the delipidation step by a casein-derived peptide NPWDQ, which was shown to be highly specific occludin inducer in epithelial cells in a previous study (Yasumatsu and Tanabe 2010). The stimulation of the occludin expression in the ex vivo porcine epidermis was confirmed by qRT-PCR and IHC showing its broader distribution in the epidermis (Figure 9b and 9c). The NPWDQ peptide treatment of the ex vivo porcine epidermis resulted in a faster decrease of the TEWL when compared to control. TEWL of the NPWDQ treated model was significantly lower than control model 120 hours after the delipidation (Figure 9a).

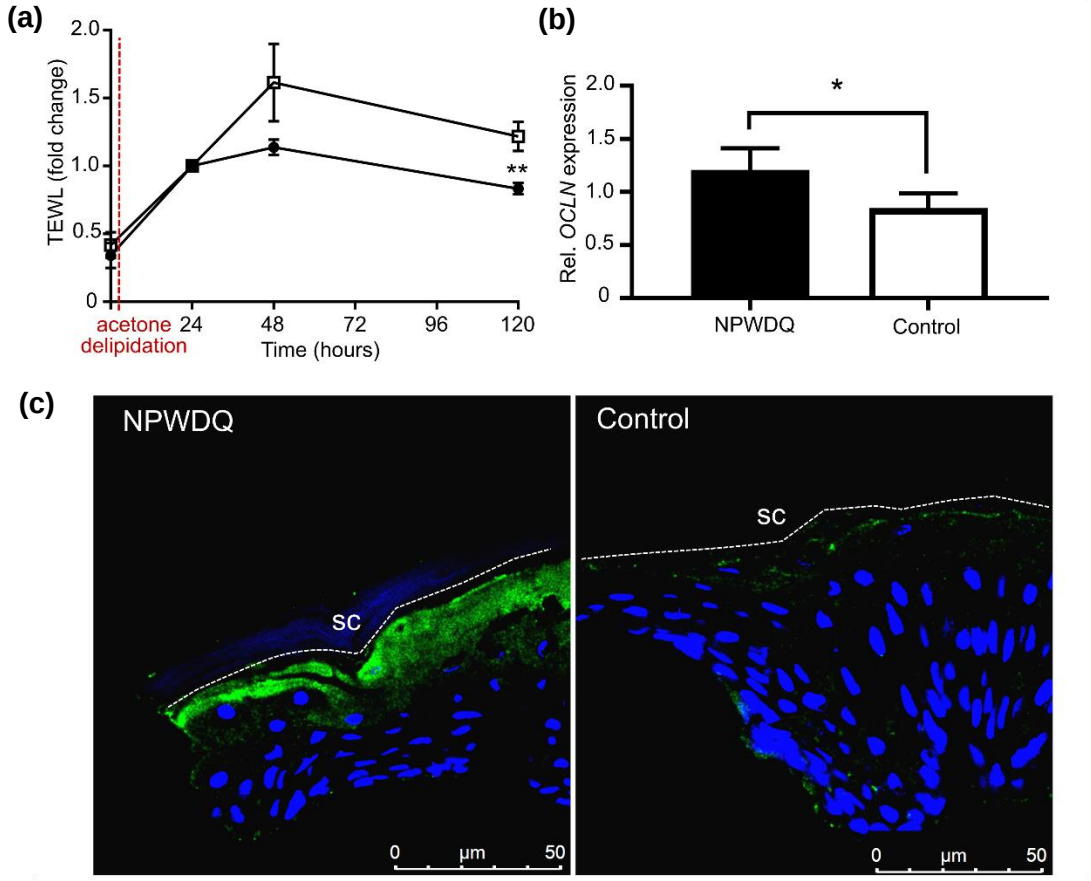

Figure 9: Casein-derived peptide NPWDQ treatment *resulted in occludin overexpression and faster TEWL restoration in ex vivo porcine epidermis after acetone delipidation. Ex vivo porcine epidermis specimens placed in modified Franz diffusion cells were delipidated using acetone and after 24 hours treated with 1.6 µM NPWDQ solution for 96 hours. (a) TEWL was monitored during the experiment using an open-chamber method at following timepoints: prior acetone delipidation (0 hours), and 24, 48 and 120 hours after acetone delipidation. The data are expressed as fold change (TEWL 24 hours after damage=1) and shown as mean ± SEM. (b) Occludin expression in the NPWDQ treated model and control 120 hours after acetone delipidation assessed by qRT-PCR (data shown as mean ± SEM; n=5) and IHC (representative images are shown; n=5; green – occludin, blue – cell nuclei, bar=50 µm). Statistical significance *P < 0.05, **P < 0.001. SC, stratum corneum.*

5 Discussion

The skin is an inhomogeneous organ whose various parameters differ both inter-individually and intra-individually. Therefore, a selection of adequate skin sites is crucial when dealing with skin analysis. SB and TS are promising less-invasive alternatives than punch biopsy, which cause permanent damage. Since both SB and TS, are not widely used for epidermal analysis, method optimization and characterization of the sample acquired was done prior to any other analysis.

Co-extraction with a phenol-based reagent (RNAzol) enables a reliable extraction of both, RNA and proteins from the same sample, and reduces an amount of the sample needed. RNAzol manufacturer's protocol had to be enhanced and used with QIAcube automated extractor to maximize the yield of both proteins and RNA. Addition of chloroform to phenol-based reagent may be useful when extracting RNA only (Reimann et al. 2019), but hampered further protein extraction in our case. For IHC detection only antibodies with experimentally verified functionality were used. Regarding the approach, we preferred frozen specimens with acetone fixation, which provided better outcomes of TJ proteins detection than paraffin embedded specimens with heat antigen retrieval.

Number of studies utilized shotgun lipidomics on various biological samples such as human blood plasma without prior HPLC separation using various approaches (e.g. ESI-QqQ, ESI-QTOF, ESI-Orbitrap, MALDI-TOF). We analyzed lipid profile in porcine epidermis using MALDI-Orbitrap and conventional DHB, CHCA and AA matrixes. Although over 100 m/z were identified with 30 m/z potentially belonging to ceramides, none of the ceramide species were confirmed due to significant mass overlap. As discussed elsewhere, MALDI approach is lacking reproducibility and fact that there is no universal matrix (Hsu 2018).

SB and TS represent different samples to work with; therefore, a different approach is needed. The duration of TS depends on the number of strips used. We also noticed that the duration of the SB sampling varied from individual to individual more than in TS. Panoutsopoulou et al. implied that the duration of SB is too long for a routine usage in the clinical practice as his team reported duration necessary to form a blister 47-85 minutes on the calf, 63-158 minutes on the foot (Panoutsopoulou et al. 2009), 42-129 minutes on distal thigh and 63-193 minutes on distal leg (Panoutsopoulou et al. 2015). Other groups reported 90-120 minutes on upper inner arm (Benfeldt et al. 1999; Leitch et al. 2016). This time is, indeed, tolerable in research laboratories, though the unpredictability of the time necessary to form a blister is rather inconvenient.

A SB roof is the sole epidermis. Therefore, no special approach is needed. TS generally provides a lesser amount of material which, in addition, is stuck to the glue of the strip hindering whole extraction process. Probably, a certain amount of the material was not detached from a sticky surface of the TS discs. Still, our yield of RNA that was roughly 300 ng from 30 TS discs is more than other groups have reported as their total RNA yield was 0.92 ng using four tape strips on the healthy skin (Wong et al. 2004) and 11 ng using twelve tape strips on the forearm (Wong et al. 2006). Nevertheless, the RNA concentration from the TS samples was too low to perform a reliable qRT-PCR analysis. Therefore, isolated RNA from the TS samples was amplified to yield a sufficient amount

of RNA (Fig. 1c). With regard to the protein yield, Clausen et al. reported approximate amount <1 µg (Clausen et al. 2013) and later 10 µg of protein per a D-Squame disc (Clausen et al. 2016), and our protein amount per a TS disc was 1.1 ± 0.13 µg on average. However, our extraction protocol was designed to extract both RNA and proteins in one procedure. During the extraction, the RNAzol® reagent caused swelling of the glue, which might have rendered the extraction of RNA and proteins more difficult. Moreover, Clausen et al. did not clearly state a diameter of the D-Squame discs and a total amount of material sampled by TS, which also might have caused the difference.

Furthermore, representative proteins of different epidermal layers were analyzed by WB and qRT-PCR: filaggrin/FLG for the SC, occludin/OCLN for the SG, claudin-1/CLDN1 for all living epidermal cell layers, laminin/LAMA3 for the stratum basale, and GAPDH/RPL13A as the housekeepers.

Although filaggrin present in the TS samples may have been sampled from the SG layer, neither claudin-1 nor occludin, which reside in the SG layer (Yuki et al. 2011), have been detected. Therefore, filaggrin that is present in the lower SC (Nachat et al. 2005) was rather obtained by TS. Upper layers of the SC do not contain filaggrin as showed by other investigators (Egawa et al. 2013). Images by RCM are congruent with our results from qRT-PCR and WB as they indicated that the SG was reached but not obtained by TS. Taken together, our results do not provide any direct evidence of collecting SG cells, rather the opposite.

The question is whether it is possible to detach living layers of the epidermis by TS. Pinkus et al. observed by light microscopy a missing SG layer in a cross-section of the skin that was biopsied after TS with a Scotch tape, but it was not confirmed with a complete certainty (Pinkus 1952). According to the literature, the SG layer starts 15-20 µm below the skin surface (Puig et al. 2012). Since the biological material obtained by TS rapidly decreased with increasing depth of the epidermis, we may anticipate that the SG is hardly obtainable even with larger amounts of tape-strips. Other studies that have used different tape-strips reached the SG using 50-70 tape-strips with a non-linear decrease of obtained material as well (Jacobi et al. 2005; Lademann et al. 2012; Weigmann et al. 1999). As far as we know, no study has ever confirmed a successful yield of a human granular layer by TS up to date. A humid surface and increasing cohesion of the SC layers towards the living epidermis decreases the effectiveness of the TS (Chapman et al. 1991; Weigmann et al. 1999).

Although proteins from all layers of the epidermis were detected in the SB samples, there is one major shortcoming of the SB technique for the epidermal analysis. Early studies characterizing the SB sampling found that the epidermis is detached from the dermis at the interface between the lamina lucida and lamina densa, leaving the lamina densa and its components attached to the dermis. Therefore, SB samples provide incomplete information about the basal membrane of the epidermis. Some of the proteins such as collagen type IV were not present in the epidermis obtained by SB (Oikarinen et al. 1982) and laminin expression was visible on a dermal as well as epidermal side after SB (Saksela et al. 1981). Alongside the qRT-PCR and WB analyses, we were also able to successfully perform IHC and lipid analyses on the same SB samples.

IR spectroscopy of the SB samples showed the presence of highly ordered SC lipids and the co-existence of a very tight orthorhombic chain with slightly looser hexagonal lipid packing, which is consistent with the literature (Boncheva et al. 2008). A simple lipid/protein ratio for comparative purpose between samples could be obtained by a ratio of the intensity of methylene symmetric stretching and Amide I band. IR spectroscopy is non-destructive and enables further sample processing, in our case, the lipid extraction and analysis. HPTLC analysis showed the presence of all barrier lipids in correct proportions (8 ceramide subclasses, free fatty acids, cholesterol and cholesteryl sulfate) and their precursors (sphingomyelins, glucosylceramides and phospholipids (PL)) (Schreiner et al. 2000). Interestingly, decreased PL were observed in the SB samples, which could be caused by their secretion into the blister fluid or their degradation and consequent secretion of degradation products into the blister fluid. PL are precursors for many bioactive lipid mediators involved in the skin inflammation and immunity response (Kendall and Nicolaou 2013). Lysophosphatidic acid had been detected in the blister fluid in higher concentration than in plasma, which suggested that lysophosphatidic acid is produced in the blister fluid by LPLD-dependent hydrolysis of lysophosphatidylcholine (Mazereeuw-Hautier et al. 2005). Also, similarities between lipid profiles in the blister fluid and epidermis indicated a primarily epidermal origin of the SB fluid (Kendall et al. 2015).

IHC and lipid analyses are performable on the TS samples as well (Camera et al. 2010; Jungersted et al. 2013; van Smeden et al. 2011), but reliable results from all the used methods are hardly achievable from a single TS sampling due to lack of material and a highly demanding workup. Indeed, multiple TS can provide enough of material. However, IHC on a single strip provides only limited information in contrast to the typical vertical cross-sections covering the whole epidermis obtained from SB. Therefore, one would have to analyze all the consecutive strips to gain complete information about the whole SC. Moreover, TS discs may not provide optimal optical conditions for microscopy and may cause non-specific binding or auto-fluorescence. For these reasons, we do find a TS sample rather unsuitable for IHC.

Also, it should be noted that both methods cause a certain level of the irritation or damage that triggers respective cellular responses during the procedure. Therefore, some of the molecules such as early immune response markers can be significantly affected even within 60 minutes of either SB or TS sampling procedure. After all, a low PL content was found in our SB samples. This should be taken into a consideration when selecting an application of SB and TS. When all outcomes of the characterization were taken into account, SB was chosen for our further study as the epidermal sampling technique.

The unimpaired water barrier in the aged skin has been an unexplained phenomenon for over years. A comprehensive meta-analysis shows that TEWL remains the same or rather decreases with age. Authors further explained this by a decreased water diffusion coefficient due to the overall reduction of lipids in the aged skin (Kottner et al. 2013b). However, the epidermis has been shown to reduce TEWL even if the SC is completely missing (Celli et al. 2012; Malminen et al. 2003). TJs represent a potential key player as they compensate for the impaired skin barrier function after the acute damage (Svoboda et al. 2016). Identification of TJ proteins induced by the skin photoaging and

the evidence of their direct link to the water barrier led to a hypothesis that TJs proteins, especially occludin, might contribute to the maintenance (or even decrease) of TEWL in the photoaged or intrinsically aged skin.

Next part of the research was focused on analysis of the human lipid composition, TEWL rates and TJ proteins expression in the young and aged skin, both the sun-protected and sun-exposed. Selected sun-exposed and sun-protected zones of the aged and young skin were confirmed to have respective typical structural features (Ganceviciene et al. 2012). Skin barrier analysis confirmed a stable water barrier in both aged skin areas, and revealed the deteriorated lipid content in the photoaged skin but not in the intrinsically aged skin suggesting a detrimental effect of the UV irradiation on the skin barrier lipid content, which is consistent with (Bak et al. 2011). However, no significant changes were detected in the ceramide subclasses. In spite of the generally accepted idea of the aged skin lacking 30% of ceramides, the literature on this matter is inconsistent (Coderch et al. 2003). Some studies do report the decrease of ceramides in the skin barrier as a function of age (Imokawa et al. 1991; Rogers et al. 1996; Schreiner et al. 2000) but this is not supported by other studies (Mutanu Jungersted et al. 2010; De Paepe et al. 2004; Sadowski et al. 2017). Clearly, there are changes in the lipid composition during the skin aging. However, other factors such as gender, site or seasons appear to have an impact on the lipid composition of the SC as well, making the results throughout the literature hardly comparable. Thus, the only trend pronounced almost in all studies is the decrease of the overall SC lipid content.

Further analysis of the skin barrier revealed significant differences in the TJ proteins expression between the young and aged skin. We observed the significant occludin overexpression that was present only in the photoaged skin, where the decreased lipid content was also found. Our results do not reconcile with a recent work, where a decreased expression of occludin was observed in the aged skin and no difference in the occludin expression between sun-exposed and sun-protected skin sites. However, young donors were rather middle aged (range 26-31years). Moreover, the comparison of sun-exposed and sun-protected involved different skin sites, buttock and forearm (Jin et al. 2016). A decreased occludin expression was also detected in squamous cell carcinoma but not in its precursor states such as the chronically sun-exposed skin (Rachow et al. 2013). Occludin as a transmembrane protein contributes to the epidermal barrier function (Furuse et al. 1993). Although its knockdown decreased the transepithelial resistance in cultured cells (Kirschner et al. 2013), no fatal TEWL phenotype was seen in mice lacking occludin. On the other hand, the occludin overexpression was detected in the regenerating human epidermis, which was accompanied with the gradually ameliorating water barrier (Malminen et al. 2003). The occludin expression was also found to be increased 3 days after an exposure to the UVB irradiation which was followed by a skin barrier improvement (Yamamoto et al. 2008). This compensation-like overexpression of occludin was also observed in the developing fetal epidermis (Celli et al. 2012) or infected epidermis (Ohnemus et al. 2008). However, to the best of our knowledge, the direct link of occludin to the water barrier (TEWL) has never been confirmed. Therefore, we utilized the ex vivo porcine epidermal model to address this issue. By using the acetone delipidation and the stimulation of occludin by a casein-derived peptide, NPWDQ, we demonstrated that the occludin overexpression contributes to the restoration of the water barrier in the skin with an impaired lipid

barrier, which is a typical feature of the photoaged skin as well. Taken together, these results suggest that occludin is an important molecule in the maintenance of the water barrier of the photoaged skin. The peptide retained its functionality in the epidermis and enhanced the water barrier on the level of TEWL. Previously, the NPWDQ peptide was shown to enhance the barrier in epithelial cells by upregulating the occludin expression (Tanabe 2012).

From other TJ proteins, claudin-1 is the most characterized. Acute UV exposure studies lead to an increase of claudin-1 on the protein level 3 days after the exposure (Yamamoto et al. 2008). Other investigators reported a decrease of claudin-1 in the aged skin. Claudin-1 null mice exhibited fatal TEWL rates (Furuse et al. 2002) and aberrant SC (Sugawara et al. 2013; Yuki et al. 2013). However, our results of the claudin-1 expression were inconsistent since mRNA levels of claudin-1 were increased in the photoaged skin whereas on the protein levels it showed rather a decrease suggesting a post-translational regulation. Therefore, we suggest that claudin-1 probably does not play a significant role in the water barrier maintenance in the photoaged skin.

ZO-2 is a scaffolding protein of TJs whose function is associated with the establishment and fine tuning of TJs (Shin and Margolis 2006). However, information on ZO-2 and its involvement in the epidermal barrier is scarce. Attenuation of ZO-2 along with ZO-1 induced by miRNA-146a and miRNA-106b has been shown to diminish the water barrier (Roy et al. 2014). Our results suggest that the intrinsic aging process rather than photoaging causes the elevation of the ZO-2 expression in the skin. Is the ZO-2 overexpression in the intrinsically aged skin important for a skin barrier integrity? ZO-2 seems to be an interesting target for future studies regarding the skin barrier.

6 Conclusion

In summary, we established a methodological basis for dermatological research in the field of the skin barrier and tight junctions in Contipro a.s. Theoretical part is focused on a state-of-the-art of analytic methods and procedures used in dermatological research and thorough review of TJs role in the skin barrier. This brought us before unchallenged hypothesis "Could tight junctions regulate barrier function of the aged skin?"

To answer this hypothesis several methods and models were developed and optimized. Suction blistering has shown itself as a valuable tool for epidermal sampling, being painless, reproducible technique and providing intact epidermal samples at the same time. Although skin represents one of the toughest and most complex organic samples, the protein/RNA co-extraction has been successfully resolved and utilized for further experiments. IHC procedure has been optimized for use with CLSM that provided us with ultra-quality images and reliable quantification of fluorescent signal via a photon counter. A conventional "gold -standard" HPTLC has been used to analyze lipid composition. MS based approach was far too time-consuming as it would require a development of whole new protocol and post-analysis processing of results, which was not an objective of this project. But, MS based analysis of epidermal lipids is one of the potential future directions of this research.

Next part of the project dealt directly with the hypothesis suggesting an important role of TJ in the maintenance of TEWL in the aged skin. Clinical aspect of the protocol has been carefully designed to ensure the safety and well-being of volunteers. Microarray analysis of aged vs young skin shown significant differences in the expression of TJ proteins. Our experiments confirmed unchanged/reduced TEWL in the aged skin and detrimental effect of photoaging on the skin lipid content in our volunteers. Further experiments demonstrated that occludin overexpression was associated with faster recovery of the water barrier in the delipidated porcine epidermis suggesting a role of occludin and TJs in the epidermis with the impaired lipid content which is a typical feature of the photoaged skin as well. Whether the maintenance of the water barrier is mediated directly by occludin creating a physical barrier or indirectly by other mechanisms warrants further studies. Furthermore, modifications of occludin such as phosphorylation or ubiquitination were shown to be essential for the barrier permeability (Murakami et al. 2009).

Despite the common epithelial character of the intestine and epidermal tissues, further studies are needed to confirm the specificity of NPWDQ towards TJs proteins and occludin in our model and the skin as such. Furthermore, occludin seems to be a promising target for the treatment of the perturbed skin barrier. Other inducers of the occludin overexpression can be tested as well. Apart from occludin, claudin-1 and ZO-2, there are also other TJ proteins worth investigating such as cingulin, claudin-6 or claudin-7 whose expression in aged skin significantly differed from young skin as shown by microarray analysis. However, knowledge of their connection to skin barrier function is rather limited. Also, as mentioned above, MS based analysis of epidermal lipids could help identify potential disturbances in lipid species profile, which conventional HPTLC fail to show.

List of References

Bak H, Hong S phil, Jeong SK, Choi EH, Lee SE, Lee SH, Sung-Ku A. Altered epidermal lipid layers induced by long-term exposure to suberythemal-dose ultraviolet. *Int. J. Dermatol.* 2011;50(7):832–7

Benfeldt E, Serup Jø, Menné T. Microdialysis vs. suction blister technique for in vivo sampling of pharmacokinetics in the human dermis. *Acta Derm. Venereol.* 1999;79(5):338–42

Bleck O, Abeck D, Ring J, Hoppe U, Vietzke JP, Wolber R, Brandt O, Schreiner V. Two ceramide subfractions detectable in Cer(AS) position by HPTLC in skin surface lipids of non-lesional skin of atopic eczema. *J. Invest. Dermatol*. 1999;113(6):894–900

Bligh EG, Dyer WJ. A rapid Method of total Lipid extraction and purification. *Can. J. Biochem. Physiol.* 1959;37(8):911–7

Boncheva M, Damien F, Normand V. Molecular organization of the lipid matrix in intact Stratum corneum using ATR-FTIR spectroscopy. *Biochim. Biophys. Acta - Biomembr.* 2008;1778(5):1344–55

Camera E, Ludovici M, Galante M, Sinagra J-L, Picardo M. Comprehensive analysis of the major lipid classes in sebum by rapid resolution high-performance liquid chromatography and electrospray mass spectrometry. J. Lipid Res. 2010b;51(11):3377–88

Celli A, Zhai Y, Jiang YJ, Crumrine D, Elias PM, Feingold KR, Mauro TM. Tight junction properties change during epidermis development. *Exp. Dermatol*. 2012;21(10):798–801

Chapman SJ, Walsh A, Jackson SM, Friedmann PS. Lipids, proteins and corneocyte adhesion. *Arch. Dermatol. Res*. 1991;283(3):167–73

Clausen ML, Jungersted JM, Andersen PS, Slotved HC, Krogfelt KA, Agner T. Human β-defensin-2 as a marker for disease severity and skin barrier properties in atopic dermatitis. *Br J Dermatol.* 2013;169(3):587–93

Clausen M-L, Slotved H-C, Krogfelt KA, Agner T. Tape Stripping Technique for Stratum Corneum Protein Analysis. *Sci. Rep.* 2016;6:19918

Coderch L, L??pez O, De La Maza A, Parra JL. Ceramides and skin function. Am. J. Clin. Dermatol. 2003;4(2):107–29

Egawa G, Doi H, Miyachi Y, Kabashima K. Skin tape stripping and cheek swab method for a detection of filaggrin. *J. Dermatol. Sci.* 2013;69(3):263–5

Elias PM. Stratum corneum defensive functions: An integrated view. *J. Invest. Dermatol*. 2005;125(2):183–200

Farage MA, Miller KW, Elsner P, Maibach HI. Functional and physiological characteristics of the aging skin. *Aging Clin. Exp. Res*. 2008;20(4):195–200

Furuse M, Hata M, Furuse K, Yoshida Y, Haratake A, Sugitani Y, et al. Claudin-based tight junctions are crucial for the mammalian epidermal barrier: A lesson from claudin-

1-deficient mice. *J. Cell Biol.* 2002;156(6):1099–111

Furuse M, Hirase T, Itoh M, Nagafuchi A, Yonemura S, Tsukita S, et al. Occludin: A novel integral membrane protein localizing at tight junctions. *J. Cell Biol*. 1993;123(6 II):1777–88

Ganceviciene R, Liakou AI, Theodoridis A, Makrantonaki E, Zouboulis CC. Skin anti-aging strategies. *Dermatoendocrinol.* 2012;4(3)

Gilchrest BA. Photoaging. *J. Invest. Dermatol.* 2013;133:E2–6

Gupta S, Shroff S, Gupta S. Modified technique of suction blistering for epidermal grafting in vitiligo. *Int. J. Dermatol.* 1999;38(4):306–9

Hsu F-F. Mass spectrometry based shotgun lipidomics-a critical review from the technical point of view. *Anal. Bioanal. Chem.* 2018;410(25):6387–6409

Hung CF, Fang CL, Al-Suwayeh SA, Yang SY, Fang JY. Evaluation of drug and sunscreen permeation via skin irradiated with UVA and UVB: Comparisons of normal skin and chronologically aged skin. *J. Dermatol. Sci.* 2012;68(3):135–48

Imokawa G, Abe A, Jin K, Higaki Y, Kawashima M, Hidano A. Decreased Level of Ceramides in Stratum Corneum of Atopic Dermatitis: An Etiologic Factor in Atopic Dry Skin? *J. Invest. Dermatol.* 1991;96(4):523–6

Jacobi U, Weigmann H-J, Ulrich J, Sterry W, Lademann J. Estimation of the relative stratum corneum amount removed by tape stripping. *Ski. Res Technol.* 2005;11(10):91–6

Jiang SJ, Chu AW, Lu ZF, Pan MH, Che DF, Zhou XJ. Ultraviolet B-induced alterations of the skin barrier and epidermal calcium gradient. *Exp. Dermatol*. 2007;16(12):985–92

Jin SP, Han SB, Kim YK, Park EE, Doh EJ, Kim KH, Lee DH, Chung JH. Changes in tight junction protein expression in intrinsic aging and photoaging in human skin in vivo. *J. Dermatol. Sci.* 2016;84:99–101

Jungersted JM, Bomholt J, Bajraktari N, Hansen JS, Klærke DA, Pedersen PA, Hedfalk K, Nielsen KH, Agner T, Hélix-Nielsen C. In vivo studies of aquaporins 3 and 10 in human stratum corneum. *Arch. Dermatol. Res*. 2013;305(8):699–704

Kendall AC, Nicolaou A. Bioactive lipid mediators in skin inflammation and immunity. *Prog. Lipid Res.* 2013;52(1):141–64

Kendall AC, Pilkington SM, Massey K a, Sassano G, Rhodes LE, Nicolaou A. Distribution of Bioactive Lipid Mediators in Human Skin. *J. Invest. Dermatol.* 2015;135(6):1510–20

Kirschner N, Rosenthal R, Furuse M, Moll I, Fromm M, Brandner JM. Contribution of Tight Junction Proteins to Ion , Macromolecule , and Water Barrier in Keratinocytes. *J. Invest. Dermatol.* 2013;133(5):1161–9

Kohl E, Steinbauer J, Landthaler M, Szeimies RM. Skin ageing. *J. Eur. Acad. Dermatology Venereol.* 2011;25(8):873–84

Kottner J, Hillmann K, Fimmel S, Seité S, Blume-Peytavi U. Characterisation of epidermal regeneration in vivo: a 60-day follow-up study. *J. Wound Care*. 2013a;22(8):395–400

Kottner J, Lichterfeld A, Blume-Peytavi U. Transepidermal water loss in young and aged healthy humans: A systematic review and meta-analysis. *Arch. Dermatol. Res*. 2013b;305(4):315–23

Kováčik A, Opálka L, Šilarová M, Roh J, Vávrová K. Synthesis of 6-hydroxyceramide using ruthenium-catalyzed hydrosilylation–protodesilylation. Unexpected formation of a long periodicity lamellar phase in skin lipid membranes. *RSC Adv*. 2016;6(77):73343–50

Lademann J, Ilgevicius a, Zurbau O, Liess HD, Schanzer S, Weigmann HJ, Antoniou C, von Pelchrzim R, Sterry W. Penetration studies of topically applied substances: Optical determination of the amount of stratum corneum removed by tape stripping. *J. Biomed. Opt.* 2012;11(5):054026

Leitch CS, Natafji E, Yu C, Abdul-Ghaffar S, Madarasingha N, Venables ZC, Chu R, Fitch PM, Muinonen-Martin AJ, Campbell LE, McLean WHI, Schwarze J, Howie SEM, Weller RB. Filaggrin-null mutations are associated with increased maturation markers on Langerhans cells. *J. Allergy Clin. Immunol.* 2016;138(2):482-490.e7

Livak KJ, Schmittgen TD. Analysis of Relative Gene Expression Data Using Real-Time Quantitative PCR and the 2−ΔΔCT Method. *Methods*. 2001;25(4):402–8

Luebberding S, Krueger N, Kerscher M. Skin physiology in men and women: In vivo evaluation of 300 people including TEWL, SC hydration, sebum content and skin surface pH. *Int. J. Cosmet. Sci*. 2013a;35(5):477–83

Luebberding S, Krueger N, Kerscher M. Age-related changes in skin barrier function - Quantitative evaluation of 150 female subjects. *Int. J. Cosmet. Sci.* 2013b;35(2):183–90

Malminen M, Koivukangas V, Peltonen J, Karvonen SL, Oikarinen A, Peltonen S. Immunohistological distribution of the tight junction components ZO-1 and occludin in regenerating human epidermis. *Br. J. Dermatol.* 2003;149(2):255–60

Mazereeuw-Hautier J, Gres S, Fanguin M, Cariven C, Fauvel J, Perret B, Chap H, Salles JP, Saulnier-Blache JB. Production of lysophosphatidic acid in blister fluid: Involvement of a lysophospholipase D activity. *J. Invest. Dermatol*. 2005;125(3):421–7

Murakami T, Felinski EA, Antonetti DA. Occludin phosphorylation and ubiquitination regulate tight junction trafficking and vascular endothelial growth factor-induced permeability. *J. Biol. Chem*. 2009;284(31):21036–46

Mutanu Jungersted J, Hellgren LI, Høgh JK, Drachmann T, Jemec GBE, Agner T. Ceramides and barrier function in healthy skin. *Acta Derm. Venereol*. 2010;90(4):350–3

Nachat R, Méchin M-C, Takahara H, Chavanas S, Charveron M, Guy S, et al. Peptidylarginine Deiminase Isoforms 1–3 Are Expressed in the Epidermis and Involved

in the Deimination of K1 and Filaggrin. *J. Invest. Dermatol.* 2005;124:384–93

Nischal U, Nischal K, Khopkar U. Techniques of skin biopsy and practical considerations. *J. Cutan. Aesthet. Surg.* 2008;1(2):107

Ohnemus U, Kohrmeyer K, Houdek P, Rohde H, Wladykowski E, Vidal S, Horstkotte MA, Aepfelbacher M, Kirschner N, Behne MJ, Moll I, Brandner JM. Regulation of Epidermal Tight-Junctions (TJ) during Infection with Exfoliative Toxin-Negative Staphylococcus Strains. *J. Invest. Dermatol.* 2008;128(4):906–16

Oikarinen A, Savolainen ER, Tryggvason K, Foidart JM, Kiistala U. Basement membrane components and galactosylhydroxylysyl glucosyltransferase in suction blisters of human skin. *Br. J. Dermatol.* 1982;106(3):257–66

Opálka L, Kováčik A, Sochorová M, Roh J, Kuneš J, Lenčo J, Vávrová K. Scalable Synthesis of Human Ultralong Chain Ceramides. *Org. Lett.* 2015;17(21):5456–9

De Paepe K, Houben E, Adam R, Wiessemann F, Rogiers V. Validation of the VapoMeter, a closed unventilated chamber system to assess transepidermal water loss vs. the open chamber Tewameter®. *Ski. Res. Technol.* 2005;11(1):61–9

Panoutsopoulou IG, Luciano CA, Wendelschafer-Crabb G, Hodges JS, Kennedy WR. Epidermal innervation in healthy children and adolescents. *Muscle and Nerve.* 2015;51(3):378–84

Panoutsopoulou IG, Wendelschafer-Crabb G, Hodges JS, Kennedy WR. Skin blister and skin biopsy to quantify epidermal nerves: A comparative study. *Neurology*. 2009;72(14):1205–10

Pinkus H. Examination of the Epidermis By the Strip Method II. Biometric Data on Regeneration of the Human Epidermis. *J. Invest. Dermatol.* 1952;19:431–47

Pouillot A, Dayan N, Polla AS, Polla LL, Polla BS. The stratum corneum: A double paradox. *J. Cosmet. Dermatol*. 2008;7(2):143–8

Proksch E, Brandner JM, Jensen JM. The skin: An indispensable barrier. *Exp. Dermatol*. 2008;17(12):1063–72

Puig S, Carrera C, Salerni G, Rocha-Portela J. Epidermis, dermis and epidermal appendages. In: Hofmann-Wellenhof R, Pellacani G, Malvehy J, Soyer HP. *Reflectance Confocal Microscopy for Skin Diseases*. Berlin: Springer; 2012. p. 21–31; ISBN: 978-3-642-21996-2.

Rachow S, Zorn-Kruppa M, Ohnemus U, Kirschner N, Vidal-y-Sy S, von den Driesch P, Börnen C, Eberle J, Mildner M, Vettorazzi E, Rosenthal R, Moll I, Brandner JM. Occludin Is Involved in Adhesion, Apoptosis, Differentiation and Ca^{2+}-Homeostasis of Human Keratinocytes: Implications for Tumorigenesis. *PLoS One*. 2013;8(2)

Reimann E, Abram K, Kõks S, Kingo K, Fazeli A. Identification of an optimal method for extracting RNA from human skin biopsy, using domestic pig as a model system. *Sci. Rep*. 2019;9(1):1–10

Rissmann R, Oudshoorn MHM, Hennink WE, Ponec M, Bouwstra JA. Skin barrier

disruption by acetone: Observations in a hairless mouse skin model. *Arch. Dermatol. Res.* 2009;301(8):609–13

Rogers J, Harding C, Mayo A, Banks J, Rawlings A. Stratum corneum lipids: The effect of ageing and the seasons. *Arch. Dermatol. Res*. 1996;288(12):765–70

Roy S, Elgharably H, Sinha M, Ganesh K, Chaney S, Mann E, et al. Mixed-species biofilm compromises wound healing by disrupting epidermal barrier function. *J. Pathol.* 2014;233(4):331–43

Sadowski T, Klose C, Gerl MJ, Wójcik-Maciejewicz A, Herzog R, Simons K, Reich A, Surma MA. Large-scale human skin lipidomics by quantitative, high-throughput shotgun mass spectrometry. *Sci. Rep.* 2017;7:43761

Saksela O, Alitalo K, Knstala U, Aheri A V. Basal Lamina Components in Experimentally Induced Skin Blisters. *J. Invest. Dermatol.* 1981;77:283–6

Sandby-Møller J, Poulsen T, Wulf HC. Epidermal Thickness at Different Body Sites: Relationship to Age, Gender, Pigmentation, Blood Content, Skin Type and Smoking Habits. *Acta Derm. Venereol.* 2003;83(6):410–3

Schreiner V, Gooris GS, Pfeiffer S, Lanzendo G, Wenck H, Diembeck W. Barrier Characteristics of Different Human Skin Types Investigated with X-Ray Diffraction, Lipid Analysis, and Electron Microscopy Imaging. *J.Invest Dermatol.* 2000;114(1994):654–60

Serup Jø, Jemec GBE, Grove GL. *Handbook of Non-Invasive Methods and the Skin. 2nd ed*. Boca Raton: CRC Press; 2006. ISBN: 9780849314377

Shah H, Rawal Mahajan S. Photoaging: New insights into its stimulators, complications, biochemical changes and therapeutic interventions. *Biomed. Aging Pathol*. 2013;3(3):161–9

Shin K, Margolis B. ZOning out Tight Junctions. *Cell.* 2006;126(4):647–9

van Smeden J, Hoppel L, van der Heijden R, Hankemeier T, Vreeken RJ, Bouwstra JA. LC/MS analysis of stratum corneum lipids: ceramide profiling and discovery. *J. Lipid Res*. 2011;52(6):1211–21

Sugawara T, Iwamoto N, Akashi M, Kojima T, Hisatsune J, Sugai M, Furuse M. Tight junction dysfunction in the stratum granulosum leads to aberrant stratum corneum barrier function in claudin-1-deficient mice. *J. Dermatol. Sci.* 2013;70(1):12–8

Svoboda M. *Adaptation of conventional and modern non-invasive methods for analysis of photoaged human skin barrier*. Pardubice; 2020.

Svoboda M, Bílková Z, Muthný T. Could tight junctions regulate the barrier function of the aged skin? *J. Dermatol. Sci.* 2016. p. 147–52

Svoboda M, Hlobilová M, Marešová M, Sochorová M, Kováčik A, Vávrová K, Dolečková I. Comparison of suction blistering and tape stripping for analysis of epidermal genes, proteins and lipids. *Arch. Dermatol. Res*. 2017; 309:757–765

Tagami H. Location-related differences in structure and function of the stratum corneum

with special emphasis on those of the facial skin. *Int. J. Cosmet. Sci*. 2008;30(6):413-34

Tanabe S. Short Peptide Modules for Enhancing Intestinal Barrier Function. *Curr. Pharm. Des*. 2012;18(6):776–81

Vávrová K, Henkes D, Strüver K, Sochorová M, Skolová B, Witting MY, Friess W, Schreml S, Meier RJ, Schäfer-Korting M, Fluhr JW, Küchler S. Filaggrin deficiency leads to impaired lipid profile and altered acidification pathways in a 3D skin construct. *J. Invest. Dermatol*. 2014;134(3):746–53

Vinson J, Anamandla S. Comparative topical absorption and antioxidant effectiveness of two forms of coenzyme q10 after a single dose and after long-term supplementation in the skin of young and middle-aged subjects. *Int. J. Cosmet. Sci*. 2006;28(2):148

Wallmeyer L, Lehnen D, Eger N, Sochorová M, Opálka L, Kováčik A, Vávrová K, Hedtrich S. Stimulation of PPARα normalizes the skin lipid ratio and improves the skin barrier of normal and filaggrin deficient reconstructed skin. *J. Dermatol. Sci*. 2015;80(2):102–10

Weigmann HJ, Lademann J, Meffert H, Schaefer H, Sterry W. Determination of the horny layer profile by tape stripping in combination with optical spectroscopy in the visible range as a prerequisite to quantify percutaneous absorption. *Skin Pharmacol. Appl. Skin Physiol*. 1999;12(1–2):34–45

Wong R, Tran V, Morhenn V, Hung SP, Andersen B, Ito E, et al. Use of RT-PCR and DNA microarrays to characterize RNA recovered by non-invasive tape harvesting of normal and inflamed skin. J. Invest. Dermatol. 2004;123(1):159–67

Wong R, Tran V, Morhenn V, Hung SP, Andersen B, Ito E, Hatfield GW, Benson NR. Use of RT-PCR and DNA microarrays to characterize RNA recovered by non-invasive tape harvesting of normal and inflamed skin. *J. Invest. Dermatol.* 2004;123(1):159–67

Yamamoto T, Kurasawa M, Hattori T, Maeda T, Nakano H, Sasaki H. Relationship between expression of tight junction-related molecules and perturbed epidermal barrier function in UVB-irradiated hairless mice. *Arch. Dermatol. Res.* 2008;300(2):61–8

Yasumatsu H, Tanabe S. The casein peptide Asn-Pro-Trp-Asp-Gln enforces the intestinal tight junction partly by increasing occludin expression in Caco-2 cells. *Br. J. Nutr.* 2010;104(7):951–6

Yuki T, Hachiya A, Kusaka A, Sriwiriyanont P, Visscher MO, Morita K, et al. Characterization of Tight Junctions and Their Disruption by UVB in Human Epidermis and Cultured Keratinocytes. *J. Invest. Dermatol.* 2011;131(3):744–52

Yuki T, Haratake A, Koishikawa H, Morita K, Miyachi Y, Inoue S. Tight junction proteins in keratinocytes: Localization and contribution to barrier function. *Exp. Dermatol.* 2007;16(4):324–30

Yuki T, Komiya A, Kusaka A, Kuze T, Sugiyama Y, Inoue S. Impaired tight junctions obstruct stratum corneum formation by altering polar lipid and profilaggrin processing. *J. Dermatol. Sci*. 2013;69(2):148–58

Zoschke C, Ulrich M, Sochorová M, Wolff C, Vávrová K, Ma N, Ulrich C, Brandner

JM, Schäfer-Korting M. The barrier function of organotypic non-melanoma skin cancer models. *J. Control. Release.* 2016;233:10–8

Zuber TJ. Punch biopsy of the skin. *Am. Fam. Physician.* 2002;65(6):1155-1158+1164+1167

List of Students' Published Works

Publication Type	Authors	Title	Publish Place	Publish Date
Original Article	Svoboda M, Hlobilová M, Marešová M, Sochorová M, Kováčik A, Vávrová K, Dolečková I	Comparison of suction blistering and tape stripping for analysis of epidermal genes, proteins and lipids	Archives of Dermatological Research IF=2.34	11/2017
Original Article	Šmejkalová D, Muthný T, Nešporová K, Hermannová M, Achbergerová E, Huerta-Angeles G, Svoboda M, Čepa M, Machalová V, Luptáková D, Velebný V	Hyaluronan Polymeric Micelles for Topical Drug Delivery	Carbohydrate Polymers IF=5.16	01/2017
Review Article	Svoboda M, Bílková Z, Muthný T	Could tight junctions regulate the barrier function of the aged skin?	Journal of Dermatological Science IF=3.73	3/2016
Presentation	Svoboda M, Dolečková I	Aged skin barrier and TEWL phenomenon	MKK 2017 Mikulov	05.10.2017
Poster	Svoboda, M, Pavlík V, Hlobilová M, Dolečková I	Expression of tight junction proteins claudin-1, occludin and ZO-2 in aged skin	ESDR 2016 Munich	07.-10.09.2016
Presentation	Svoboda, M, Pavlík V, Hlobilová M, Dolečková I	Structural analysis and relative quantification of tight junction proteins: claudin-1 in human skin biopsy using confocal microscope.	CeCe 2015 Brno	21.-23.09.2015
Poster	Svoboda M, Muthný T	Lipidomic profile of porcine epidermis by maldi-orbitrap mass spectrometry using shotgun approach.	CeCe 2015 Brno	21.-23.09.2015
Poster	Svoboda M, Salvetová E, Šmejkalová D, Muthný T	Preanalytic phase optimization of ethyl ferulate analysis after penetration experiments into the skin within various delivery systems	Cece 2014 Brno	20.-22.10.2014